Riemannian theory of Hamiltonian chaos and Lyapunov exponents

Lapo Casetti[*]

Scuola Normale Superiore, Piazza dei Cavalieri 7, 56126 Pisa, Italy

Cecilia Clementi[†]

International School for Advanced Studies (SISSA/ISAS), via Beirut 2-4, 34014 Trieste, Italy

Marco Pettini[‡]

Osservatorio Astrofisico di Arcetri, Largo E. Fermi 5, 50125 Firenze, Italy

(February 5, 2008)

Abstract

A non-vanishing Lyapunov exponent λ_1 provides the very definition of deterministic chaos in the solutions of a dynamical system, however no theoretical mean of predicting its value exists. This paper copes with the problem of analytically computing the largest Lyapunov exponent λ_1 for many degrees of freedom Hamiltonian systems as a function of $\varepsilon = E/N$, the energy per degree of freedom. The functional dependence $\lambda_1(\varepsilon)$ is of great interest because, among other reasons, it detects the existence of weakly and strongly chaotic regimes. This aim - analytic computation of $\lambda_1(\varepsilon)$ - is successfully reached within a theoretical framework that makes use of a geometrization of newtonian dynamics in the language of Riemannian differential geometry. A new point of view about the origin of chaos in these systems is obtained independently of the standard explanation based on homoclinic intersections. Dynamical instability (chaos) is here related to curvature fluctuations of the

manifolds whose geodesics are natural motions and is described by means of
Jacobi – Levi-Civita equation (JLCE) for geodesic spread. In this paper it is
shown how to derive from JLCE an effective stability equation. Under general
conditions, this effective equation formally describes a stochastic oscillator; an
analytic formula for the instability growth-rate of its solutions is worked out
and applied to the Fermi-Pasta-Ulam β-model and to a chain of coupled rota-
tors. An excellent agreement is found between the theoretical prediction and
numeric values of $\lambda_1(\varepsilon)$ for both models.

I. INTRODUCTION

During the last two decades or so, there has been a growing evidence of the independence of the two properties of *determinism* and *predictability* of classical dynamics. In fact, predictability for arbitrary long times requires also the *stability* of the motions with respect to variations – however small – of the initial conditions.

With the exception of integrable systems, the generic situation of classical dynamical systems describing, say, N particles interacting through physical potentials, is *instability* of the trajectories in the Lyapunov sense. Nowadays such an instability is called intrinsic stochasticity, or chaoticity, of the dynamics and is a consequence of nonlinearity of the equations of motion.

Likewise any other kind of instability, dynamical instability brings about the exponential growth of an initial perturbation, in this case it is the distance between a reference trajectory and any other trajectory originating in its close vicinity that *locally* grows exponentially in time. Quantitatively, the degree of chaoticity of a dynamical system is characterized by the largest Lyapunov exponent λ_1 that – if positive – measures the mean instability rate of nearby trajectories averaged along a sufficiently long reference trajectory. The exponent λ_1 also measures the typical time scale of memory loss of the initial conditions.

Let us remember that if

$$\dot{x}^i = X^i(x^1 \ldots x^N) \tag{1}$$

is a given dynamical system, i.e. a realisation in local coordinates of a one-parameter group of diffeomorphisms of a manifold M, that is of $\phi^t : M \rightarrow M$, and if we denote by

$$\dot{\xi}^i = \mathcal{J}_k^i[x(t)]\,\xi^k \tag{2}$$

the usual tangent dynamics equation, i.e. the realisation of the mapping $d\phi^t : TM \rightarrow TM$, where TM is the tangent bundle of M and $[\mathcal{J}_k^i]$ is the Jacobian matrix of $[X^i]$, then the largest Lyapunov exponent λ_1 is defined by

$$\lambda_1 = \lim_{t \to \infty} \frac{1}{t} \ln \frac{\|\xi(t)\|}{\|\xi(0)\|} \tag{3}$$

and, by setting $\Lambda[x(t), \xi(t)] = \xi^T \mathcal{J}[x(t)] \xi / \xi^T \xi \equiv \xi^T \dot{\xi} / \xi^T \xi = \frac{1}{2} \frac{d}{dt} \ln(\xi^T \xi)$, this can be formally expressed as a time average

$$\lambda_1 = \lim_{t \to \infty} \frac{1}{2t} \int_0^t d\tau \, \Lambda[x(\tau), \xi(\tau)] \quad . \tag{4}$$

Even though λ_1 is the most important indicator of chaos of classical [1] dynamical systems, it is used only as a diagnostic tool in numerical simulations. With the exception of a few simple discrete-time systems (maps of the interval), no theoretical method exists to compute λ_1 [2]. This situation reveals that a satisfactory theory of deterministic chaos is still lacking, at least for systems of physical relevance.

In the conventional theory of chaos, dynamical instability is caused by homoclinic intersections of perturbed separatrices, however this theory has many problems: *i)* it needs action-angle coordinates, *ii)* it works in conditions of weak perturbation of an integrable system, *iii)* to compute quantities like Mel'nikov integrals one needs the analytic expressions of the unperturbed separatrices: at large N this is hopeless, moreover the generalization of Poincaré-Birkhoff theorem is still problematic at $N > 2$; *iv)* finally, there is no computational relationship between homoclinic intersections and Lyapunov exponents. Therefore this theory seems not adequate to treat chaos in Hamiltonian systems with many degrees of freedom at arbitrary degree of nonlinearity, with potentials that can be hardly transformed in action-angle coordinates, not to speak of accounting for phenomena like the transition from weak to strong chaos in Hamiltonian systems [3,4]. Motivated by the need of understanding this transition from weak to strong chaos, we have recently proposed [5–10] to tackle Hamiltonian chaos in a theoretical framework different from that of homoclinic intersections. This new method makes use of the well-known possibility of formulating Hamiltonian dynamics in the language of Riemannian geometry so that the stability or instability of a geodesic flow depends on curvature properties of some suitably defined manifold.

In the early 1940s, N. S. Krylov already got a hold of the potential interest of this differential-geometric framework to account for dynamical instability and hence for phase

space mixing [11]. The follow-up of his intuition can be found in abstract ergodic theory [12] and in a very few mathematical works concerning the ergodicity of geodesic flows of physical interest [13,14]. However, Krylov's work did not entail anything useful for a more general understanding of chaos in nonlinear newtonian dynamics because one soon hits against unsurmountable mathematical obstacles. By filling certain mathematical gaps with numerical investigations, these obstacles have been overcome and a rich scenario emerged about the relationship between stability and curvature

Based on the so-obtained information, the present paper aims at bringing a substantial contribution to the development of a Riemannian theory of Hamiltonian chaos. The new contribution consists of a method to analytically compute the largest Lyapunov exponent λ_1 for physically meaningful Hamiltonian systems of arbitrary large number of degrees of freedom. A preliminary and limited account of the results presented here can be found in Ref. [7].

The paper is organized as follows: Section II is a sketchy presentation of the geometrization of newtonian dynamics; Section III contains the derivation of an effective stability equation from Jacobi – Levi-Civita equation for geodesic spread and an analytic formula for λ_1; Section IV contains the application of the general result to the practical computation of λ_1 in the Fermi-Pasta-Ulam β-model and in a chain of coupled rotators. Some concluding remarks are presented in Section V.

II. GEOMETRIZATION OF NEWTONIAN DYNAMICS

Let us briefly recall how newtonian dynamics can be rephrased in the language of Riemannian geometry. We shall deal with standard autonomous systems, i.e. described by the Lagrangian function

$$\mathcal{L} = T - V = \frac{1}{2} a_{ij} \dot{q}_i \dot{q}_j - V(q_1, \ldots, q_N) \ , \tag{5}$$

so that the Hamiltonian function $\mathcal{H} = T + V \equiv E$ is a constant of motion.

According to the principle of stationary action – in the form of Maupertuis – among all the possible isoenergetic paths $\gamma(t)$ with fixed end points, the paths that make vanish the first variation of the action functional

$$\mathcal{A} = \int_{\gamma(t)} p_i \, dq_i = \int_{\gamma(t)} \frac{\partial \mathcal{L}}{\partial \dot{q}_i} \dot{q}_i \, dt \tag{6}$$

are natural motions.

As the kinetic energy T is a homogeneous function of degree two, we have $2T = \dot{q}_i \partial \mathcal{L}/\partial \dot{q}_i$, and Maupertuis' principle reads

$$\delta \mathcal{A} = \delta \int_{\gamma(t)} 2T \, dt = 0 \ . \tag{7}$$

The configuration space M of a system with N degrees of freedom is an N-dimensional differentiable manifold and the lagrangian coordinates $(q_1, \ldots, q_N)$ can be used as local coordinates on M. The manifold M is naturally given a proper Riemannian structure. In fact, let us consider the matrix

$$g_{ij} = 2[E - V(q)] a_{ij} \tag{8}$$

so that (7) becomes

$$\delta \int_{\gamma(t)} 2T \, dt = \delta \int_{\gamma(t)} \left(g_{ij} \dot{q}^i \dot{q}^j\right)^{1/2} dt = \delta \int_{\gamma(s)} ds = 0 \ , \tag{9}$$

thus natural motions are geodesics of M, provided we define ds as its arclength. The metric tensor g_J of M is then defined by

$$g_J = g_{ij} \, dq^i \otimes dq^j \tag{10}$$

where $(dq^1, \ldots, dq^N)$ is a natural base of $T_q^* M$ - the cotangent space at the point q - in the local chart $(q^1, \ldots, q^N)$. This is known as Jacobi (or kinetic energy) metric. Denoting by ∇ the canonical Levi-Civita connection, the geodesic equation

$$\nabla_{\dot{\gamma}} \dot{\gamma} = 0 \tag{11}$$

becomes, in the local chart $(q^1, \ldots, q^N)$,

$$\frac{d^2q^i}{ds^2} + \Gamma^i_{jk}\frac{dq^j}{ds}\frac{dq^k}{ds} = 0 \ , \tag{12}$$

where the Christoffel coefficients are the components of ∇ defined by

$$\Gamma^i_{jk} = \langle dq^i, \nabla_j e_k \rangle = \frac{1}{2}g^{im}\left(\partial_j g_{km} + \partial_k g_{mj} - \partial_m g_{jk}\right) \ , \tag{13}$$

where $\partial_i = \partial/\partial q^i$. Without loss of generality consider $g_{ij} = 2[E - V(q)]\delta_{ij}$, from Eq. (12) we get

$$\frac{d^2q^i}{ds^2} + \frac{1}{2(E-V)}\left[2\frac{\partial(E-V)}{\partial q_j}\frac{dq^j}{ds}\frac{dq^i}{ds} - g^{ij}\frac{\partial(E-V)}{\partial q_j}g_{km}\frac{dq^k}{ds}\frac{dq^m}{ds}\right] = 0 \ , \tag{14}$$

and, using $ds^2 = 2(E-V)^2 \, dt^2$, we can easily verify that these equations yield

$$\frac{d^2q^i}{dt^2} = -\frac{\partial V}{\partial q_i} \quad i = 1,\dots,N \ . \tag{15}$$

which are Newton equations.

As already discussed elsewhere [5,6], there are other possibilities to associate a Riemannian manifold to a standard Hamiltonian system. Among the others we mention a structure, defined by Eisenhart [15], that will be used in the following for computational reasons. In this case the ambient space is an enlarged configuration space-time $M \times \mathbb{R}^2$, with local coordinates $(q^0, q^1, \dots, q^N, q^{N+1})$, with $(q^1, \dots, q^N) \in M$, $q^0 \in \mathbb{R}$ is the time coordinate, $q^{N+1} \in \mathbb{R}$ is a coordinate closely related to the action; Eisenhart defines a pseudo-Riemannian non-degenerate metric g_E on $M \times \mathbb{R}^2$ as

$$ds^2_E = g_{\mu\nu}\, dq^\mu \otimes dq^\nu = a_{ij}\, dq^i \otimes dq^j - 2V(q)\, dq^0 \otimes dq^0 + dq^0 \otimes dq^{N+1} + dq^{N+1} \otimes dq^0 \ . \tag{16}$$

Natural motions are now given by the canonical projection π of the geodesics of $(M \times \mathbb{R}^2, g_E)$ on configuration space-time: $\pi : M \times \mathbb{R}^2 \to M \times \mathbb{R}$. However, among all the geodesics of g_E we must consider only those for which the arclength is positive definite and given by

$$ds^2 = g_{\mu\nu}dq^\mu dq^\nu = 2C^2 dt^2 \ , \tag{17}$$

or, equivalently, we have to consider only those geodesics such that the coordinate q^{N+1} evolves according to

$$q^{N+1} = C^2 t + C_1^2 - \int_0^t \mathcal{L} \, d\tau \, , \tag{18}$$

where C and C_1 are real constants. Since the values of these constants are arbitrary, we fix $C^2 = 1/2$ in order that $ds^2 = dt^2$ along a physical geodesic. For a diagonal kinetic energy matrix $a_{ij} = \delta_{ij}$, the non vanishing components of the connection ∇ are simply

$$\Gamma_{00}^i = -\Gamma_{0i}^{N+1} = \partial_i V \, , \tag{19}$$

therefore it is easy to check that also the geodesics of g_E yield Newton equations together with the differential versions of Eq. (18) and of $q^0 = t$ (details can be found in [5,6]).

III. GEOMETRIC DESCRIPTION OF DYNAMICAL INSTABILITY

The actual interest of the Riemannian formulation of dynamics stems from the possibility of studying the instability of natural motions through the instability of geodesics of a suitable manifold, a circumstance that has several advantages. First of all a powerful mathematical tool exists to investigate the stability or instability of a geodesic flow: the Jacobi – Levi-Civita equation (JLC) for geodesic spread. The JLC equation describes covariantly how nearby geodesics locally scatter and it is a familiar object both in Riemannian geometry and theoretical physics (it is of fundamental interest in experimental General Relativity). Moreover the JLC equation relates the stability or instability of a geodesic flow with *curvature* properties of the ambient manifold, thus opening a wide and largely unexplored field of investigation of the connections among geometry, topology and geodesic instability, hence chaos.

A. Jacobi - Levi Civita equation for geodesic spread

A *congruence of geodesics* is defined as a family of geodesics $\{\gamma_\tau(s) = \gamma(s, \tau) \, | \, \tau \in \mathbb{R}\}$ that, originating in some neighbourhood $\mathcal{I}$ of any given point of a manifold, are differentiably parametrized by some parameter τ. Choose a reference geodesic $\bar{\gamma}(s, \tau_0)$, denote by $\dot{\gamma}(s)$ the

field of vectors tangent at s to $\bar{\gamma}$ and denote by $J(s)$ the field of vectors tangent at τ_0 to the curves $\gamma_s(\tau)$ at fixed s. The field $J = (\partial\gamma/\partial\tau)_{\tau_0}$ is known as *geodetic separation field* and it has the property: $\mathcal{L}_{\dot{\gamma}}J = 0$, where $\mathcal{L}$ is the Lie derivative. Locally we can measure the distance between two nearby geodesics by means of J.

The evolution of the geodetic separation field J conveys information about stability or instability of the reference geodesic $\bar{\gamma}$, in fact, if $\|J\|$ exponentially grows with s then the geodesic is unstable in the sense of Lyapunov, otherwise it is stable.

The evolution of J is described by [19]

$$\frac{\nabla^2 J(s)}{ds^2} + R(\dot{\gamma}(s), J(s))\,\dot{\gamma}(s) = 0 \ , \tag{20}$$

known as Jacobi – Levi-Civita (JLC) equation. Here $J(s) \in T_{\gamma(s)}M$; $R(X,Y) = \nabla_X\nabla_Y - \nabla_Y\nabla_X - \nabla_{[X,Y]}$ is the Riemann-Christoffel curvature tensor; $\dot{\gamma} = d\gamma/ds$; ∇/ds is the covariant derivative and $\gamma(s)$ is a normal geodesic, i.e. such that s is the length. In the following we assume that $J(s)$ is normal, i.e. $\langle J, \dot{\gamma} \rangle = 0$. This equation relates the stability or instability of nearby geodesics to the curvature properties of the ambient manifold. If the ambient manifold is endowed with a metric (e.g. Jacobi or Eisenhart) derived from the Lagrangian of a physical system, then stable or unstable (chaotic) motions will depend on the curvature properties of the manifold. Therefore it is reasonable to guess that some *average* global geometric property will provide information, at least, about an *average* degree of chaoticity of the dynamics independently of the knowledge of the trajectories, that is independently of the numerical integration of the equations of motion.

In local coordinates the JLC equation (20) reads as

$$\frac{\nabla^2 J^i}{ds^2} + R^i{}_{jkl}\frac{dq^j}{ds}J^k\frac{dq^l}{ds} = 0 \ , \tag{21}$$

where $R^i{}_{jkl} = \langle dq^i, R(e_{(k)}, e_{(l)})e_{(j)}\rangle$ are the components of the curvature tensor, and the covariant derivative is $(\nabla J^i/ds) = dJ^i/ds + \Gamma^i_{jk}J^k dq^j/ds$. There are $\mathcal{O}(N^4)$ of such components, $N = \dim M$, therefore – even if this number can be considerably reduced by symmetry considerations – equation (21) appears untractable already at rather small N. It is worth

9

mentioning that some exception exists. Such is the case of *isotropic* manifolds for which (21) can be reduced to the simple form

$$\frac{\nabla^2 J^i}{ds^2} + K J^i = 0 \quad i = 1, \ldots, N \;,\tag{22}$$

where K is the constant value assumed throughout the manifold by the sectional curvature.

The sectional curvature of a manifold is the N-dimensional generalization of the gaussian curvature of two-dimensional surfaces of $\mathbb{R}^3$. Consider two arbitrary vectors $X, Y \in T_x M$, where $x \in M$ is an arbitrary point of M, and define

$$\|X \wedge Y\| = (\|X\|^2 \|Y\|^2 - \langle X, Y \rangle)^{1/2}\tag{23}$$

if $\|X \wedge Y\| \neq 0$ the vectors X, Y span a two-dimensional plane $\pi \subset T_x M$, then the sectional curvature at x relative to the plane π is defined by

$$K(X, Y) = K(x, \pi) = \frac{\langle R(Y, X)X, Y \rangle}{\|X \wedge Y\|^2}\tag{24}$$

which is only a property of M at x independently of $X, Y \in \pi$ (Gauss' theorema egregium). For an isotropic manifold $K(x, \pi)$ is also independent of the choice of π and thus, according to Schur's theorem, K turns out also independent of $x \in M$.

Unstable solutions of the equation (22) are of the form

$$J(s) = w(0)(-K)^{-1/2} \sinh\left(\sqrt{-K}\, s\right) \;,\tag{25}$$

once the initial conditions are assigned as $J(0) = 0$ and $dJ(0)/ds = w(0)$ and $K < 0$. In abstract ergodic theory geodesic flows on compact manifolds of constant negative curvature have been considered in classical works [16]. In this case the quantity $\sqrt{-K}$ – uniform on the manifold – measures the degree of instability of nearby geodesics.

While Eq. (22) holds true only for constant curvature manifolds, a similar form of general validity can be obtained for JLC equation at $N = 2$.

In this low-dimensional case Eq. (21) is exactly rewritten as

$$\frac{d^2 J}{ds^2} + \frac{1}{2}\mathcal{R}(s)J = 0 \;,\tag{26}$$

10

where a parallely transported frame is used and $\mathcal{R}(s)$ is the scalar curvature. Using Jacobi metric one finds $(N = 2)$: $\mathcal{R} = \triangle V/W^2 + (\nabla V)^2/W^3$, with $W = E - V$, so that for smooth and binding potentials $\mathcal{R}$ can be negative only where $\triangle V < 0$, i.e nowhere for nonlinearly coupled oscillators as described by the Hénon-Heiles model [9] or for quartic oscillators [10]. $\triangle V < 0$ is only possible if the potential V has inflection points.

Recent detailed analyses of two-degrees of freedom systems [9,10] have shown that chaos can be produced by *parametric instability* due to a fluctuating positive curvature along the geodesics.

Let us remember that parametric instability is a generic property of dynamical systems with parameters that are periodically or quasi-periodically varying in time, even if for each value of the varying parameter the system has stable solutions [17]. A harmonic oscillator with periodically modulated frequency, described by the Mathieu equation, is perhaps the prototype of such a parametric instability mechanism.

Numerical simulations have shown that all the informations about order and chaos obtained by standard means (Lyapunov exponent and Poincaré sections) are fully retrieved by using Eq. (26). As in the case of tangent dynamics, Eq. (26) has to be computed along a reference geodesic (trajectory).

Let us now cope with the large N case. It is convenient to rewrite the JLC equation (21) in the following form

$$\frac{\nabla^2 J(s)}{ds^2} + \frac{1}{N-1}\left[\mathrm{Ric}(\dot{\gamma}(s),\dot{\gamma}(s))\,J(s)\;-\;\mathrm{Ric}(\dot{\gamma}(s),J(s))\,\dot{\gamma}(s)\right] + W(\dot{\gamma}(s),J(s))\,\dot{\gamma}(s) = 0\,,$$

(27)

where W is the Weyl projective curvature tensor whose components W^i_{jkl} are given by [18]

$$W^i{}_{jkl} = R^i{}_{jkl} - \frac{1}{N-1}(R_{jl}\delta^i_k - R_{jk}\delta^i_l)\,,$$

(28)

and Ric is the Ricci curvature tensor of components $R_{ij} = R^m{}_{imj}$. Weyl's projective tensor W (not to be confused with Weyl's *conformal* curvature tensor) measures the deviation from isotropy of a given manifold. For an isotropic manifold $W^i_{jkl} = 0$, and we recognize

11

in (27) equation (22), in fact in this case $R_{jl}\dot{q}^j\dot{q}^l/(N-1)$ is just the constant value of sectional curvature. Remind that the Ricci curvature at $x \in M$ is $K_R(X_{(b)}) = R_{jl}X_{(b)}^i X_{(b)}^l = \sum_{a=1}^{N-1} K(X_{(b)}, X_{(a)})$ where $X_{(1)}, \ldots, X_{(N)}$ form an orthonormal basis of T_xM. Hence we understand that Eq. (27) retains the structure of Eq. (22) up to its second term that now has the meaning of a mean sectional curvature averaged, at any given point, over the independent orientations of the planes spanned by $X_{(a)}$ and $X_{(b)}$; this mean sectional curvature is no longer constant along $\gamma(s)$. The last term of (27) accounts for the local degree of anisotropy of the ambient manifold.

Let us now consider the following decomposition for the Jacobi field J

$$J(s) = \sum_i J_i(s)\, e_{(i)}(s) \tag{29}$$

where $\{e_{(1)} \ldots e_{(N)}\}$ is an orthonormal system of parallely transported vectors. In this reference frame it is

$$\frac{\nabla^2 J}{ds^2} = \sum_i \frac{d^2 J_i}{ds^2}\, e_{(i)}(s) \tag{30}$$

and the last term of (27) is

$$
\begin{aligned}
W(\dot{\gamma}, J)\dot{\gamma} &= \sum_j \langle W(\dot{\gamma}, J)\dot{\gamma}, e_{(j)}\rangle\, e_{(j)} \\
&= \sum_j \langle W(\dot{\gamma}, \sum_i J_i e_{(i)})\dot{\gamma}, e_{(j)}\rangle\, e_{(j)} \\
&= \sum_{ij} \langle W(\dot{\gamma}, e_{(i)})\dot{\gamma}, e_{(j)}\rangle\, J_i\, e_{(j)} \ ,
\end{aligned}
\tag{31}
$$

the same decomposition applies to the third term of Eq. (27) which is finally rewritten as

$$\frac{d^2 J_j}{ds^2} + k_R(s)\, J_j + \sum_i (w_{ij} + r_{ij})\, J_i = 0 \tag{32}$$

where $k_R = K_R/(N-1)$, $w_{ij} = \langle W(\dot{\gamma}, e_{(i)})\dot{\gamma}, e_{(j)}\rangle$ and $r_{ij} = \langle \mathrm{Ric}(\dot{\gamma}, e_{(i)})\dot{\gamma}, e_{(j)}\rangle/(N-1)$. Of course k_R is independent of the coordinate system. The elements w_{ij} still depend on the dynamics and on the behavior of the vectors $e_{(k)}(s)$, thus, in order to obtain a stability equation, for the geodesic flow, that depends only on average curvature properties of the

ambient manifold, we try to conveniently approximate the w_{ij}. To this purpose define at any point $x \in M$ the trilinear mapping $R' : T_x M \times T_x M \times T_x M \to T_x M$ by

$$\langle R'(X,Y,U), Z \rangle = \langle X,U \rangle \langle Y,Z \rangle - \langle Y,U \rangle \langle X,Z \rangle \qquad (33)$$

for all $X, Y, U, Z \in T_x M$. It is well known [19] that, if and only if M is isotropic then $R = K_0 R'$, where R is the Riemann curvature tensor of M and K_0 is the constant sectional curvature.

Let us now assume that the ambient manifold is *quasi-isotropic*, i.e. that it looks like an isotropic manifold after a coarse-graining that smears out all the metric fluctuations, and let us formulate this assumption by putting $R \approx K(s)R'$ and $\mathrm{Ric} \approx K(s)g$, although $K(s)$ is no longer a constant. Now we use (33) to find $w_{ij} \approx \delta K(s)[\langle \dot\gamma, \dot\gamma \rangle \langle e_{(i)}, e_{(j)} \rangle - \langle e_{(i)}, \dot\gamma \rangle \langle \dot\gamma, e_{(j)} \rangle]$, then we use $\mathrm{Ric} \propto g$ and $g(\dot\gamma, J) = 0$ to find $r_{ij} = 0$ thus Eq. (32) becomes

$$\frac{d^2 J_j}{ds^2} + k_R(s)\, J_j + \delta K(s)\, J_j = 0 \ , \qquad (34)$$

by $\delta K(s) = K(s) - \overline{K}$ we denote the local deviation of sectional curvature from its coarse-grained value $\overline{K}$, thus $\delta K(s)$ measures the fluctuation of sectional curvature along a geodesic due to the local deviation from isotropy. The problem is that $\delta K(s)$ still depends on a moving plane $\pi(s)$ determined by $\dot\gamma(s)$ and $J(s)$. In order to get rid of this dependence, consider that if $x \in M$ is an isotropic point then the components of the Ricci tensor are $R_{lh} = (N-1)K(x)g_{lh}$ and the scalar curvature is $R = N(N-1)K(x)$; with these quantities one constructs the Einstein tensor $G_{lh} = R_{lh} - \frac{1}{2}g_{lh}R$ whose divergence vanishes identically $(G_{lh|l} = 0)$ so that it is immediately found that, if a manifold consists entirely of isotropic points, then $\partial K(x)/\partial x^l = 0$ and so $\partial K_R(x)/\partial x^l = 0$, i.e. the manifold is a space of constant curvature (Schur's theorem [19]). Conversely, the local variation of Ricci curvature detects the local loss of isotropy, thus a reasonable approximation of the *average* variation $\delta K(s)$ along a geodesic may be given by the variation of Ricci curvature.

Next let us model $\delta K(s)$ along a geodesic by a stochastic process. In fact $K(s)$ is obtained by summing a large number of terms, each one depending on different combinations

of the components of J and on the the coordinates q^i, moreover, unless we tackle an integrable model, the dynamics is always chaotic and the functions $q^i(s)$ behave irregularly. By invoking a central-limit-theorem argument, at large N, $\delta K(s)$ is expected to behave, in first approximation, as a gaussian stochastic process. More generally, the probability distribution $\mathcal{P}(\delta K)$ may be other than gaussian and in practice it could be determined by computing its cumulants along a geodesic $\gamma(s)$.

Now we make quantitative the previous statement – about using the variation of Ricci curvature along a geodesic to estimate $\delta K(s)$ – by putting

$$\mathcal{P}(\delta K) \simeq \mathcal{P}(\delta K_R) \ . \tag{35}$$

Both δK and δK_R are zero mean variations, so the first moments vanish; according to (35) the following relation for the second moments will hold

$$\langle [K(s) - \overline{K}]^2 \rangle_s \simeq \frac{1}{N-1} \langle [K_R(s) - \langle K_R \rangle_s]^2 \rangle_s \ , \tag{36}$$

where $\langle \cdot \rangle_s$ stands for proper-time average along a geodesic $\gamma(s)$. Let us comment about the numerical factor in the r.h.s. of (36) where a factor $\frac{1}{N^2}$ might be expected. At increasing N the mean square fluctuations of k_R drop to zero as $\frac{1}{N}$ because k_R is the mean of independent quantities, however this cannot be the case of the mean square fluctuations of K, in fact out of the sum K_R of all the sectional curvatures, in Eq. (34) only one sectional curvature is "picked-up" from point to point by δK so that δK remains finite with increasing N. Therefore, as the second cumulant of δK does not vanish with N, we have to keep finite the second cumulant of δK_R, what is simply achieved by properly adjusting the numerical factor in Eq. (36).

The lowest order approximation of a cumulant expansion of the stochastic process $\delta K(s)$ is the gaussian approximation

$$\delta K(s) \simeq \frac{1}{\sqrt{N-1}} \langle \delta^2 K_R \rangle_s^{1/2} \eta(s) \ , \tag{37}$$

where $\eta(s)$ is a random gaussian process with zero mean and unit variance. Finally, in order to decouple the stability equation from the dynamics, we replace time averages with static

14

averages computed with a suitable ergodic invariant measure μ. As we deal with autonomous Hamiltonian systems, a natural choice is the microcanonical measure on the constant energy surface of phase space [20]

$$\mu \propto \delta(\mathcal{H} - E) \tag{38}$$

so that Eq. (37) becomes

$$\delta K(s) \simeq \frac{1}{\sqrt{N-1}} \langle \delta^2 K_R \rangle_\mu^{1/2} \, \eta(s) \; . \tag{39}$$

Similarly, $k_R(s)$ in Eq. (34) is replaced by $\langle k_R \rangle_\mu$, in fact at large N the fluctuations of k_R – as already noticed above – vanish as $\frac{1}{N}$ because the coarse-grained manifold is isotropic, so that we finally have

$$\frac{d^2\psi}{ds^2} + \langle k_R \rangle_\mu \, \psi + \frac{1}{\sqrt{N-1}} \langle \delta^2 K_R \rangle_\mu^{1/2} \, \eta(s) \, \psi = 0 \; , \tag{40}$$

where ψ stands for any of the components J^j, since all of them now obey the same effective equation of motion. The instability growth-rate of ψ measures the instability growth-rate of $\|J\|^2$ and thus provides the dynamical instability exponent in our Riemannian framework. Equation (40) is a scalar equation which, *independently of the knowledge of dynamics*, provides a measure of the average degree of instability of the dynamics itself through the behavior of $\psi(s)$. The peculiar properties of a given Hamiltonian system enter Eq. (40) through the global geometric properties $\langle k_R \rangle_\mu$ and $\langle \delta^2 K_R \rangle_\mu$ of the ambient Riemannian manifold (whose geodesics are natural motions) and are sufficient to determine the average degree of chaoticity of the dynamics. Moreover, according to (38), $\langle k_R \rangle_\mu$ and $\langle \delta^2 K_R \rangle_\mu$ are functions of the energy E of the system – or of the energy density $\varepsilon = E/N$ which is the relevant parameter as $N \to \infty$ – so that from (40) we can obtain the energy dependence of the geometric instability exponent.

B. An analytic formula for the largest Lyapunov exponent

By transforming Eq. (20) into Eq. (40) the original complexity of the JLC equation has been considerably reduced: from a tensor equation we have worked out an effective

scalar equation formally representing a stochastic oscillator. In fact (40), with a self-evident notation, is in the form

$$\frac{d^2\psi}{ds^2} + \Omega(s)\,\psi = 0 \tag{41}$$

where $\Omega(s)$ is a gaussian stochastic process.

Now, passing from proper time s to physical time t, Eq. (41) simply reads

$$\frac{d^2\psi}{dt^2} + \Omega(t)\,\psi = 0 \quad, \tag{42}$$

where

$$\Omega(t) = \langle k_R \rangle_\mu + \frac{1}{\sqrt{N}} \langle \delta^2 K_R \rangle_\mu^{1/2}\, \eta(t) \tag{43}$$

if the Eisenhart metric is used [because of the affine parametrization of the arclength with time, Eq. (17)]; if Jacobi metric is used, we have

$$\Omega(t) = \langle k_R \rangle_\mu + \left\langle -\frac{1}{4}\left(\frac{\dot W}{W}\right)^2 + \frac{1}{2}\frac{d}{dt}\left(\frac{\dot W}{W}\right)\right\rangle_\mu + \frac{1}{\sqrt{N}} \langle \delta^2 K_R \rangle_\mu^{1/2}\, \eta(t) \tag{44}$$

[see Eq. (64) of [5] and Eq. (27) of [9]], note that $d/dt = \dot q^j(\partial/\partial q^j)$. Being interested in the large N limit, we replaced $N-1$ with N in Eqs. (43) and (44). Of course Ricci curvature has different expressions according to the metric used.

The stochastic process $\Omega(t)$ is not completely determined unless its time correlation function $\Gamma_\Omega(t_1, t_2)$ is given. We consider a stationary and δ-correlated process $\Omega(t)$ so that $\Gamma_\Omega(t_1, t_2) = \Gamma_\Omega(|t_2 - t_1|)$ and

$$\Gamma_\Omega(t) = \tau\,\sigma_\Omega^2\,\delta(t) \quad, \tag{45}$$

where τ is a characteristic time scale of the process. In order to estimate τ, let us notice that for a geodesic flow on a smooth manifold the assumption of δ-correlation of $\Omega(t)$ will be reasonable only down to some time scale below which the differentiable character of the geodesics will be felt. In other words, we have to think that in reality the power spectrum of $\Omega(t)$ is flat up to some high frequency cutoff, let us denote it by $\nu_\star$; therefore, by representing

16

the δ function as the limit for $\nu \to \infty$ of $\delta_\nu(t) = \frac{\sin(\nu t)}{\pi t}$, a more realistic representation of the autocorrelation function $\Gamma_\Omega(t)$ in Eq. (45) could be $\Gamma_\Omega^\star(t) = \sigma_\Omega^2 \frac{1}{\pi} \frac{\sin(\nu_\star t)}{\nu_\star t} \equiv \tau_\star \sigma_\Omega^2 \delta_{\nu_\star}(t)$, whence $\tau_\star = 1/\nu_\star$. Notice that $\int_{0^-}^\infty \Gamma_\Omega(t) dt = \tau \sigma_\Omega^2$ and $\int_{0^-}^\infty \Gamma_\Omega^\star(t) dt = \frac{1}{2} \tau_\star \sigma_\Omega^2$ thus $\tau = \tau_\star/2$. For practical computational reasons it is convenient to use $\Gamma_\Omega(t)$ in the form given by Eq. (45) (with the implicit assumption that $\nu_\star$ is sufficiently large), however, being $\nu_\star$ finite, the definition $\tau = \tau_\star/2$ will be kept. To estimate $\tau_\star$ we proceed as follows. A first time scale, which we will refer to as τ_1, is associated to the time needed to cover the average distance between two successive conjugate points along a geodesic [21]. In fact, at distances smaller than this one the geodesics are minimal and far from looking like random walks, whereas at each crossing of a conjugate point the separation vector field increases as if the geodesics in the local congruence were kicked (this is what happens when parametric instability is active). From Rauch's comparison theorem [19] we know that if sectional curvature K is bounded as follows: $0 < L \leq K \leq H$, then the distance d between two successive conjugate points is bounded by $\frac{\pi}{\sqrt{H}} < d < \frac{\pi}{\sqrt{L}}$. We need the lower bound estimate that, for strongly convex domains [22], is slightly modified to $d > \frac{\pi}{2\sqrt{H}}$.

Hence we define τ_1 through

$$\tau_1 = \left\langle \frac{dt}{ds} \right\rangle d_\star = \left\langle \frac{dt}{ds} \right\rangle \frac{\pi}{2\sqrt{\Omega_0 + \sigma_\Omega}} \tag{46}$$

where $\left\langle \frac{dt}{ds} \right\rangle$ is the average of the ratio between proper and physical time ($\left\langle \frac{dt}{ds} \right\rangle = 1$ if Eisenhart metric is used) and the upper bound H of K is replaced by the N-th fraction of a typical peak value of Ricci curvature, which is in turn estimated as its average Ω_0 plus the typical value δK of the (positive) fluctuation, i.e. in a gaussian approximation $\delta K = \sigma_\Omega$. This time scale is expected to be the most relevant only as long as curvature is positive and the fluctuations, compared to the average, are small.

Another time scale, referred to as τ_2, is related to local curvature fluctuations. These will be felt on a length scale of the order of, at least, $l = 1/\sqrt{\sigma_\Omega}$ (the average fluctuation of curvature radius). The scale l is expected to be relevant one when the fluctuations are of the same order of magnitude as the average curvature. When the sectional curvature is positive

17

(resp. negative), lengths and time intervals – on a scale l – are enlarged (resp. shortened) by a factor $(l^2 K/6)$ [23], so that the period $\frac{2\pi}{\sqrt{\Omega_0}}$ has a fluctuation amplitude d_2 given by $d_2 = \frac{l^2 K}{6} \frac{2\pi}{\sqrt{\Omega_0}}$; replacing K by its most probable value Ω_0 one gets

$$\tau_2 = \left\langle \frac{dt}{ds} \right\rangle d_2 = \left\langle \frac{dt}{ds} \right\rangle \frac{l^2 \Omega_0}{6} \frac{2\pi}{\sqrt{\Omega_0}} \simeq \left\langle \frac{dt}{ds} \right\rangle \frac{\Omega_0^{1/2}}{\sigma_\Omega} \ . \tag{47}$$

Finally τ in Eq. (45) is obtained by combining τ_1 with τ_2 as follows

$$\tau^{-1} = 2\tau_\star^{-1} = 2\left(\tau_1^{-1} + \tau_2^{-1}\right) \ . \tag{48}$$

The present estimate of τ is very close – though not equal – to the one of Ref. [7].

Whenever $\Omega(t)$ in Eq. (42) has a non-vanishing stochastic component the solution $\psi(t)$ has an exponentially growing envelope [24] whose growth-rate provides a measure of the degree of chaoticity. Let us call this quantity Lyapunov exponent and denote it by λ. In the next Section we shall make more precise the relationship of λ with the conventional largest Lyapunov exponent.

Our exponent λ is defined as

$$\lambda = \lim_{t\to\infty} \frac{1}{2t} \log \frac{\psi^2(t) + \dot\psi^2(t)}{\psi^2(0) + \dot\psi^2(0)} \ , \tag{49}$$

where $\psi(t)$ is solution of Eq. (42).

The ratio $(\psi^2(t) + \dot\psi^2(t))/(\psi^2(0) + \dot\psi^2(0))$ is computed by means of a technique, developed by Van Kampen and sketched in Appendix A, which is based on the possibility of computing analytically the evolution of the second moments of ψ and $\dot\psi$, averaged over the realizations of the stochastic process, from

$$\frac{d}{dt} \begin{pmatrix} \langle \psi^2 \rangle \\ \langle \dot\psi^2 \rangle \\ \langle \psi\dot\psi \rangle \end{pmatrix} = \begin{pmatrix} 0 & 0 & 2 \\ 2\sigma_\Omega^2 \tau & 0 & -2\Omega_0 \\ -\Omega_0 & 1 & 0 \end{pmatrix} \begin{pmatrix} \langle \psi^2 \rangle \\ \langle \dot\psi^2 \rangle \\ \langle \psi\dot\psi \rangle \end{pmatrix} \tag{50}$$

where Ω_0 and σ_Ω are respectively the mean and the variance of $\Omega(t)$ above defined. By diagonalizing the matrix in the r.h.s. of (50) one finds two complex conjugate eigenvalues,

18

and one real eigenvalue related to the evolution of $\frac{1}{2}\left(\langle\psi^2\rangle + \langle\dot\psi^2\rangle\right)$. According to (49) the exponent λ is half the real eigenvalue. Simple algebra leads to the final expression

$$\lambda(\Omega_0, \sigma_\Omega, \tau) = \frac{1}{2}\left(\Lambda - \frac{4\Omega_0}{3\Lambda}\right), \tag{51a}$$

$$\Lambda = \left(2\sigma_\Omega^2\tau + \sqrt{\left(\frac{4\Omega_0}{3}\right)^3 + (2\sigma_\Omega^2\tau)^2}\right)^{1/3}. \tag{51b}$$

All the quantities Ω_0, σ_Ω and τ can be computed as *static* averages, therefore – within the validity limits of the assumptions made above – Eqs. (51) provide an analytic formula to compute the largest Lyapunov exponent independently of the numerical integration of the dynamics and of the tangent dynamics.

1. Lyapunov exponent and Eisenhart metric

Let us consider dynamical systems described by the Lagrangian function (5) with a diagonal kinetic energy matrix, i.e. $a_{ij} = \delta_{ij}$, and let us choose as ambient manifold the enlarged configuration space-time equipped with the Eisenhart metric (16).

Trivial algebra gives $\Gamma_{00}^i = (\partial V/\partial q_i)$ and $\Gamma_{0i}^{N+1} = (-\partial V/\partial q^i)$ as the only nonvanishing Christoffel coefficients and hence the Riemann curvature tensor has only the following nonvanishing components

$$R_{0i0j} = \frac{\partial^2 V}{\partial q^i \partial q^j}. \tag{52}$$

The JLC equation (20) is thus rewritten in local coordinates as

$$\frac{\nabla}{ds}\frac{\nabla}{ds}J^0 + R_{i0j}^0\frac{dq^i}{ds}J^0\frac{dq^j}{ds} + R_{0ij}^0\frac{dq^0}{ds}J^i\frac{dq^j}{ds} = 0$$

$$\frac{\nabla}{ds}\frac{\nabla}{ds}J^i + R_{0j0}^i\left(\frac{dq^0}{ds}\right)^2 J^j + R_{00j}^i\frac{dq^0}{ds}J^0\frac{dq^j}{ds} + R_{j00}^i\frac{dq^j}{ds}J^0\frac{dq^0}{ds} = 0$$

$$\frac{\nabla}{ds}\frac{\nabla}{ds}J^{N+1} + R_{i0j}^{N+1}\frac{dq^i}{ds}J^0\frac{dq^j}{ds} + R_{ij0}^{N+1}\frac{dq^i}{ds}J^j\frac{dq^0}{ds} = 0. \tag{53}$$

As $\Gamma_{ij}^0 = 0$ implies $\nabla J^0/ds = dJ^0/ds$ and as $R_{ijk}^0 = 0$, we find that the first of these equations reads

$$\frac{d^2 J^0}{ds^2} = 0 \ , \tag{54}$$

hence J^0 does not accelerate and, without loss of generality, we can set $\dot{J}^0(0) = J^0(0) = 0$, this yields (using $\nabla J^i/ds = dJ^i/ds + \Gamma^i_{0k}\dot{q}^0 J^k + \Gamma^i_{k0}\dot{q}^k J^0$)

$$\frac{\nabla^2 J^i}{ds^2} = \frac{d^2 J^i}{ds^2} \tag{55}$$

and the second equation in (53) gives, for the projection in configuration space of the separation vector,

$$\frac{d^2 J^i}{ds^2} + \frac{\partial^2 V}{\partial q_i \partial q_k}\left(\frac{dq^0}{ds}\right)^2 J_k = 0 \qquad i = 1, ..., N; \tag{56}$$

the third of equations (53) describes the passive evolution of J^{N+1} which does not contribute the norm of J because $g_{N+1N+1} = 0$, so we can disregard it.

As already mentioned in the previous Section, along the physical geodesics of g_E it is $ds^2 = (dq^0)^2 = dt^2$ therefore Eq. (56) is exactly the usual tangent dynamics equation reported in the Introduction, provided that the obvious identification $\xi = (\xi_q, \xi_p) \equiv (J, \dot{J})$ is made. This clarifies the relationship between the geometric description of the instability of a geodesic flow and the conventional description of dynamical instability. It has been recently shown [9,10] that the solutions of the equations (56) and (26) (where $\mathcal{R}$ is computed with Jacobi metric) are strikingly close one another in the case of two degrees of freedom systems. This result is reasonable because the geodesics of $(M \times \mathbb{R}^2, g_E)$ – that are natural motions – project themselves onto the geodesics of (M, g_J), and as the extra coordinates q^0 and q^{N+1} do not contribute to the instability of the geodesic flow , both local and global instability properties must be the same with either Jacobi or Eisenhart metrics, independently of N.

With Eisenhart metric the only nonvanishing component of the Ricci tensor is $R_{00} = \triangle V$, where $\triangle$ is the euclidean Laplacian in configuration space. Hence Ricci curvature is $k_R(q) = \triangle V/(N-1)$ (remember that we choose the constant C such that $ds^2 = dt^2$ along a physical geodesic) and the stochastic process $\Omega(t)$ in (42) is specified by

$$\Omega_0 = \langle k_R \rangle_\mu = \frac{1}{N}\langle \triangle V \rangle_\mu \ , \tag{57a}$$

20

$$\sigma_\Omega^2 = \frac{1}{N}\langle\delta^2 K_R\rangle_\mu = \frac{1}{N}\left(\langle(\triangle V)^2\rangle_\mu - \langle\triangle V\rangle_\mu^2\right) \tag{57b}$$

$$2\tau = \frac{\pi\sqrt{\Omega_0}}{2\sqrt{\Omega_0(\Omega_0 + \sigma_\Omega)} + \pi\sigma_\Omega} \quad . \tag{57c}$$

2. Averages of geometric quantities

Let us now sketch how to compute the mean and the variance of any observable function $f(q)$, a geometric quantity of the chosen ambient manifold, by means of the microcanonical measure (38), i.e.

$$\langle f(q)\rangle_\mu = \frac{1}{\omega_E}\int f(q)\,\delta(\mathcal{H}(q,p) - E)\,dq\,dp \tag{58}$$

where

$$\omega_E = \int \delta(\mathcal{H}(q,p) - E)\,dq\,dp \tag{59}$$

and $q = (q_1 \ldots q_N)$, $p = (p_1 \ldots p_N)$. By using the configurational partition function $Z_C(\beta)$, given by

$$Z_C(\beta) = \int dq\,e^{-\beta V(q)} \tag{60}$$

where $dq = \prod_{i=1}^N dq_i$, we can compute the Gibbsian average $\langle f\rangle^G$ of the observable f as

$$\langle f\rangle^G = [Z_C(\beta)]^{-1}\int dq\,f(q)\,e^{-\beta V(q)} \quad . \tag{61}$$

Whenever this average is known, we can obtain the microcanonical average of f [27] in the following parametric form

$$\langle f\rangle_\mu(\varepsilon) \rightarrow \begin{cases} \langle f\rangle_\mu(\beta) = \langle f\rangle^G(\beta) \\ \\ \varepsilon(\beta) = \dfrac{1}{2\beta} - \dfrac{1}{N}\dfrac{\partial}{\partial\beta}[\log Z_C(\beta)] \ . \end{cases} \tag{62}$$

By replacing f with the explicit expression for Ricci curvature $k_R = \frac{1}{N} K_R$ we can work out Ω_0. Notice that Eq. (62) is strictly valid in the thermodynamic limit; at finite N it is

$$\langle f \rangle_\mu(\beta) = \langle f \rangle^G(\beta) + \mathcal{O}(\tfrac{1}{N}).$$

At variance with the computation of $\langle f \rangle$, which is insensitive to the choice of the probability measure in the $N \to \infty$ limit, computing the fluctuations of f, i.e. of $\langle \delta^2 f \rangle = \frac{1}{N}\langle (f - \langle f \rangle)^2 \rangle$, by means of the canonical or microcanonical measures yields different results. The relationship between the canonical – i.e. computed with the Gibbsian weight $e^{-\beta \mathcal{H}}$ – and the microcanonical fluctuations is given by the well known formula [27]

$$\langle \delta^2 f \rangle_\mu(\varepsilon) = \langle \delta^2 f \rangle^G(\beta) - \frac{\beta^2}{C_V} \left[\frac{\partial \langle f \rangle^G(\beta)}{\partial \beta} \right]^2, \tag{63}$$

where

$$C_V = -\frac{\beta^2}{N} \frac{\partial \langle E \rangle}{\partial \beta} \tag{64}$$

is the specific heat at constant volume and $\beta = \beta(\varepsilon)$ is given in implicit form by the second equation in (62).

By replacing f with k_R we can work out σ_Ω^2.

IV. APPLICATIONS

In this Section the Riemannian approach to Hamiltonian chaos described above is practically used to compute $\lambda_1(\varepsilon)$ for two different models: the Fermi-Pasta-Ulam (FPU) β-model and a chain of coupled rotators.

The choice of these models is motivated by the possibility of analytically computing, in the $N \to \infty$ limit, the geometric quantities needed, and by their interest as mentioned in the following subsections.

A. The Fermi-Pasta-Ulam β-model

The FPU β-model is defined by the Hamiltonian [25]

22

$$\mathcal{H}(p,q) = \sum_{i=1}^{N} \frac{1}{2} p_i^2 + \sum_{i=1}^{N} \left[\frac{1}{2} (q_{i+1} - q_i)^2 + \frac{\mu}{4} (q_{i+1} - q_i)^4 \right] . \tag{65}$$

This is a paradigmatic model of nonlinear classical many-body systems that has been extensively studied over the last decades and that stimulated remarkable developments in nonlinear dynamics, one example: the discovery of solitons. For a recent review we refer to [26]. Also the transition between weak and strong chaos has been first discovered in this model [3,4] and then, the effort of understanding the origin of such a threshold has stimulated the development of the geometric theory presented here.

Let us now compute the average Ricci curvature Ω_0 and its fluctuations σ_Ω. We have seen above that, using Eisenhart metric, k_R is given by

$$k_R = \frac{1}{N} \sum_{i=1}^{N} \frac{\partial^2 V(q)}{\partial q_i^2} , \tag{66}$$

for the FPU β-model this reads

$$k_R = 2 + \frac{6\mu}{N} \sum_{i=1}^{N} (q_{i+1} - q_i)^2 , \tag{67}$$

note that k_R is always positive.

In order to compute the Gibbsian average of k_R and its fluctuations, we rewrite the configurational partition function as

$$\tilde{Z}_C(\alpha) = \int_{-\infty}^{+\infty} \prod_{i=1}^{N} dq_i \exp \left\{ -\beta \sum_{i=1}^{N} \left[\frac{\alpha}{2} (q_{i+1} - q_i)^2 + \frac{\mu}{4} (q_{i+1} - q_i)^4 \right] \right\} , \tag{68}$$

which, in terms of the arbitrary parameter α and of Z_C, is expressed as $\tilde{Z}_C(\alpha) = Z_C(\alpha\beta, \mu/\alpha)$ and leads to the following identity

$$\langle k_R \rangle(\beta) = 2 - \frac{12\mu}{\beta N} \frac{1}{Z_C} \left[\frac{\partial}{\partial \alpha} \tilde{Z}_C(\alpha) \right]_{\alpha=1} . \tag{69}$$

Thus we have to compute

$$\frac{1}{N Z_C} \left[\frac{\partial}{\partial \alpha} \tilde{Z}_C(\alpha) \right]_{\alpha=1} = \frac{1}{N} \left[\frac{\partial}{\partial \alpha} \log \tilde{Z}_C(\alpha) \right]_{\alpha=1} \tag{70}$$

using

$$\tilde{Z}_C(\alpha) = [\tilde{z}_C(\alpha)]^N f(\alpha) , \tag{71}$$

where $f(\alpha)$ is a quantity $\mathcal{O}(1)$, $\tilde{z}_C(\alpha)$ is the single particle partition function [28]

$$\tilde{z}_C(\alpha) = \Gamma\left(\frac{1}{2}\right)\left(\frac{\beta\mu}{2}\right)^{-1/4} \exp(\frac{1}{4}\alpha^2\theta^2)D_{-1/2}(\alpha\theta) , \tag{72}$$

Γ is the Euler function, $D_{-1/2}$ is a parabolic cylinder function and

$$\theta = \left(\frac{\beta}{2\mu}\right)^{1/2} . \tag{73}$$

The final result in parametric form of the average Ricci curvature of $(M \times \mathbb{R}^2, g_E)$ – with the constant energy constraint – is (details can be found in [6])

$$\Omega_0(\varepsilon) \to \begin{cases} \langle k_R \rangle(\theta) = 2 + \dfrac{3}{\theta}\dfrac{D_{-3/2}(\theta)}{D_{-1/2}(\theta)} \\[2em] \varepsilon(\theta) = \dfrac{1}{8\sigma}\left[\dfrac{3}{\theta^2} + \dfrac{1}{\theta}\dfrac{D_{-3/2}(\theta)}{D_{-1/2}(\theta)}\right] \end{cases} \tag{74}$$

Let us now compute

$$\sigma_\Omega^2(\varepsilon) = \frac{1}{N}\langle \delta^2 K_R \rangle_\mu(\varepsilon) = \frac{1}{N}\langle (K_R - \langle K_R \rangle)^2 \rangle_\mu . \tag{75}$$

According to Eq. (63), first the Gibbsian average of this quantity, $\langle \delta^2 k_R \rangle^G(\beta) = \frac{1}{N}\langle (K_R - \langle K_R \rangle)^2 \rangle^G(\beta)$, has to be computed and then the correction term must be added. Now define

$$Q = \sum_{i=1}^{N}(q_{i+1} - q_i)^2 ; \tag{76}$$

after Eq. (67),

$$\frac{1}{N}\langle \delta^2 K_R \rangle^G(\beta) = \frac{1}{N}\langle (K_R - \langle K_R \rangle)^2 \rangle^G = \frac{36\mu^2}{N}\langle (Q - \langle Q \rangle)^2 \rangle^G , \tag{77}$$

hence using Eq. (68)

$$\langle (Q - \langle Q \rangle)^2 \rangle^G = \frac{4}{\beta^2}\left[\frac{\partial^2}{\partial\alpha^2} \log \tilde{Z}_C(\alpha)\right]_{\alpha=1} , \tag{78}$$

and finally

24

$$\frac{1}{N}\langle\delta^2 K_R\rangle^G = \frac{144\mu^2}{\beta^2}\left[\frac{\partial^2}{\partial\alpha^2}\log\tilde{z}_C(\alpha)\right]_{\alpha=1}. \tag{79}$$

Simple algebra gives

$$\left[\frac{\partial^2}{\partial\alpha^2}\log\tilde{z}_C(\alpha)\right]_{\alpha=1} = \frac{\theta^2}{4}\left\{2 - 2\theta\frac{D_{-3/2}(\theta)}{D_{-1/2}(\theta)} - \left[\frac{D_{-3/2}(\theta)}{D_{-1/2}(\theta)}\right]^2\right\}, \tag{80}$$

so that from Eq. (79) we obtain

$$\frac{1}{N}\langle\delta^2 K_R\rangle^G(\theta) = \frac{9}{\theta^2}\left\{2 - 2\theta\frac{D_{-3/2}(\theta)}{D_{-1/2}(\theta)} - \left[\frac{D_{-3/2}(\theta)}{D_{-1/2}(\theta)}\right]^2\right\}. \tag{81}$$

According to the prescription of Eq. (63), the final result for the fluctuations of Ricci curvature is

$$\sigma_\Omega^2(\varepsilon) \rightarrow \begin{cases} \dfrac{1}{N}\langle\delta^2 K_R\rangle_\mu(\theta) = \dfrac{1}{N}\langle\delta^2 K_R\rangle^G(\theta) - \dfrac{\beta^2}{c_V(\theta)}\left(\dfrac{\partial\langle k_R\rangle(\theta)}{\partial\beta}\right)^2 \\[4mm] \varepsilon(\theta) = \dfrac{1}{8\mu}\left[\dfrac{3}{\theta^2} + \dfrac{1}{\theta}\dfrac{D_{-3/2}(\theta)}{D_{-1/2}(\theta)}\right] \end{cases} \tag{82}$$

where $\langle\delta^2 K_R\rangle^G(\theta)$ is given by (81), the derivative part of the correction term is

$$\frac{\partial\langle k_R\rangle(\theta)}{\partial\beta} = \frac{3}{8\mu\theta^3}\frac{\theta D_{-3/2}^2(\theta) + 2(\theta^2-1)D_{-1/2}(\theta)D_{-3/2}(\theta) - 2\theta D_{-1/2}^2(\theta)}{D_{-1/2}^2(\theta)}, \tag{83}$$

and the specific heat per particle c_V is found to be

$$c_V(\theta) = \frac{1}{16 D_{-1/2}^2(\theta)}\left\{(12 + 2\theta^2)D_{-1/2}^2(\theta) + 2\theta D_{-1/2}(\theta)D_{-3/2}(\theta) \right.$$
$$\left. - \theta^2 D_{-3/2}(\theta)\left[2\theta D_{-1/2}(\theta) + D_{-3/2}(\theta)\right]\right\}. \tag{84}$$

The microcanonical averages in Eqs.(74) and (82) are compared in Figs. 1 and 2 with their corresponding time averages computed along numerical trajectories of the model (65) at $N = 128$ and $N = 512$ with $\mu = 0.1$. The equations of motion are integrated using a third order bilateral symplectic algorithm [29] which is a high precision numerical scheme.

Though microcanonical averages are computed in the thermodynamic limit, the agreement between time and ensemble averages is excellent already at $N = 128$.

Now we use (74) and (82) to compute τ according to its definition in (57c), then we substitute $\Omega_0(\varepsilon)$, $\sigma_\Omega^2(\varepsilon)$ and $\tau(\varepsilon)$ into Eq. (51) to obtain the analytic prediction for $\lambda_1(\varepsilon)$ in the limit $N \to \infty$. In Fig. 3 this analytic result is compared to the numeric values of λ_1 computed by means of the standard algorithm [30] at $N = 256$ and $N = 2000$ with $\mu = 0.1$ and at different ε. The agreement between analytic and numeric results is strikingly good.

B. A chain of coupled rotators

Let us now consider the system described by the Hamiltonian

$$\mathcal{H}(p, q) = \sum_{i=1}^{N} \left\{ \frac{p_i^2}{2} + J[1 - \cos(q_{i+1} - q_i)] \right\}. \tag{85}$$

If the canonical coordinates q_i and p_i are given the meaning of angular coordinates and momenta, this Hamiltonian describes a linear chain of N rotators constrained to rotate on a plane and coupled by a nearest-neighbor interaction.

This model can be formally obtained by restricting to one spatial dimension the classical Heisenberg model whose potential energy is $V = -J \sum_{\langle i,j \rangle} \mathbf{S}_i \cdot \mathbf{S}_j$, where the sum is extended only over nearest-neighbor pairs, J is the coupling constant and each $\mathbf{S}_i$ has unit module and rotates on a plane. To each "spin" $\mathbf{S}_i = (\cos q_i, \sin q_i)$ the velocity $\frac{d}{dt}\mathbf{S}_i = (-\frac{dq_i}{dt} \sin q_i, \frac{dq_i}{dt} \cos q_i)$ is associated so that (85) follows from $\mathcal{H} = \sum_{i=1}^{N} \frac{1}{2}\dot{\mathbf{S}}_i^2 - J \sum_{\langle i,j \rangle} \mathbf{S}_i \cdot \mathbf{S}_j$.

The Hamiltonian (85) has two integrable limits. In the limit of vanishing energy it represents a chain of harmonic oscillators

$$\mathcal{H}(p, q) \simeq \sum_{i=1}^{N} \left\{ \frac{p_i^2}{2} + J(q_{i+1} - q_i)^2 \right\}, \tag{86}$$

whereas in the limit of indefinitely growing energy a system of freely rotating objects is found because of potential boundedness.

The expression of Ricci curvature K_R, computed with Eisenhart metric, is

$$K_R = \sum_{i=1}^{N} \frac{\partial^2 V(q)}{\partial q_i^2} = 2J \sum_{i=1}^{N} \cos(q_{i+1} - q_i). \tag{87}$$

Let us observe that for this model a relation exists between potential energy V and Ricci curvature K_R:

$$V(q) = JN - \frac{K_R}{2}. \tag{88}$$

This relation binds the fluctuating quantity that enters the analytic formula for λ_1. This constraint does not exist for the sectional curvature thus a-priori it may be expected that some problem will arise.

The configurational partition function for a chain of coupled rotators is

$$
\begin{aligned}
Z_C(\beta) &= \int_{-\pi}^{\pi} \prod_{i=1}^{N} dq_i \exp\left\{ -\beta \sum_{i=1}^{N} J[1 - \cos(q_{i+1} - q_i)] \right\} \\
&= \exp(-\beta JN) \int_{-\pi}^{\pi} \prod_{i=1}^{N} d\omega_i \exp(\beta J \sum_{i=1}^{N} \cos \omega_i) \\
&= \exp(-\beta\, JN)[I_0(\beta\, J)]^N (2\pi)^N g(\overline{\omega}) \ .
\end{aligned}
\tag{89}
$$

where $I_0(x) = \frac{1}{\pi} \int_0^{+\pi} e^{x \cos\theta} d\theta$ is the modified Bessel function of index zero; $\omega_i = q_{i+1} - q_i$, $i \in (1, \dots, N-1)$, $\omega_N = \overline{q} - q_N$, $\overline{q} = \overline{\omega}$ depend on the initial conditions. The function $g(\overline{\omega})$ contributes with a term of $\mathcal{O}(\frac{1}{N})$ thus vanishing in the thermodynamic limit.

In order to compute Ω_0 and σ_Ω^2 we follow the same procedure adopted for the FPU model, i.e. we define

$$
\begin{aligned}
\tilde{Z}_C(\alpha) &= \int_{-\pi}^{+\pi} \prod_{i=1}^{N} dq_i \exp\left\{ -\beta \sum_{i=1}^{N} [1 - \alpha \cos(q_{i+1} - q_i)] \right\} \\
&= \exp(-\beta JN) \left[I_0(\beta J \alpha) \right]^N g(\overline{\omega})(2\pi)^N
\end{aligned}
\tag{90}
$$

and by observing that

$$\langle k_R \rangle_\mu (\beta) = \frac{2}{N\beta} \left[\frac{\partial}{\partial\alpha} \log \tilde{Z}_C(\alpha) \right]_{\alpha=1}. \tag{91}$$

we find $\Omega_0(\varepsilon)$ in parametric form

$$\Omega_0(\varepsilon) \rightarrow \begin{cases} \langle k_R \rangle_\mu(\beta) = 2J \dfrac{I_0(\beta J)}{I_1(\beta J)} \\[2em] \varepsilon(\beta) = \dfrac{1}{2\beta} + J\left(1 - \dfrac{I_1(\beta J)}{I_0(\beta J)}\right). \end{cases} \tag{92}$$

In order to work out the average of the square fluctuations of Ricci curvature we use the following identity

$$\frac{1}{N}\langle \delta^2 K_R \rangle^G = \frac{4}{\beta^2 N}\left[\frac{\partial^2}{\partial \alpha^2} \log \tilde{Z}_C(\alpha)\right]_{\alpha=1} \tag{93}$$

whence

$$\frac{1}{N}\langle \delta^2 K_R \rangle^G = 4J^2 \frac{\beta J I_0^2(\beta J) - I_1(\beta J)I_0(\beta J) - \beta J I_1^2(\beta J)}{\beta J I_0^2(\beta J)}. \tag{94}$$

The computation of the correction term $\left[\frac{\partial \langle k_R \rangle(\beta)}{\partial \beta}\right]^2 / \frac{\partial \varepsilon(\beta)}{\partial \beta}$ involves the following derivatives

$$\frac{\partial \varepsilon(\beta)}{\partial \beta} = -\frac{1}{2\beta} - J^2 \left\{ 1 - \frac{1}{\beta J}\frac{I_1(\beta J)}{I_0(\beta J)} - \left[\frac{I_1(\beta J)}{I_0(\beta J)}\right]^2 \right\} \tag{95}$$

$$\frac{\partial \langle k_R \rangle(\beta)}{\partial \beta} = 2J^2 \left\{ 1 - \frac{1}{\beta J}\frac{I_1(\beta J)}{I_0(\beta J)} - \left[\frac{I_1(\beta J)}{I_0(\beta J)}\right]^2 \right\}. \tag{96}$$

Finally, gluing together the different terms, we obtain

$$\sigma_\Omega^2(\varepsilon) \rightarrow \begin{cases} \dfrac{1}{N}\langle \delta^2 K_R \rangle(\beta) = \dfrac{4J}{\beta} \dfrac{\beta J I_0^2(\beta J) - I_0(\beta J)I_1(\beta J) - \beta J I_1^2(\beta J)}{I_0^2(\beta J)\left[1 + 2(\beta J)^2\right] - 2\beta J I_1(\beta J)I_0(\beta J) - 2\left[\beta J I_1(\beta J)\right]^2} \\[2em] \varepsilon(\beta) = \dfrac{1}{2\beta} + J\left[1 - \dfrac{I_1(\beta J)}{I_0(\beta J)}\right]. \end{cases} \tag{97}$$

In Figs. 4 and 5 the comparison between analytic and numeric results is provided for the average Ricci curvature and its fluctuations. The agreement between ensemble and time averages is very good. Time averages are computed along numerical trajectories of the model Hamiltonian (85) at $N = 150$ and $J = 1$. The already mentioned high precision symplectic algorithm has been used also in this case.

By inserting into Eq. (51) the analytic expressions of $\Omega_0(\varepsilon)$ and $\sigma_\Omega^2(\varepsilon)$ given in Eqs. (92) and (97) – and also $\tau(\varepsilon)$ which is a function of the latter quantities – we find $\lambda_1(\varepsilon)$.

In Fig. 6 the comparison is given between the analytic result so obtained and the outcome of numeric computations performed with the standard algorithm [30]. Figure 6 shows that there is agreement between analytic and numeric values of the largest Lyapunov exponent only at low and high energy densities. Likewise the FPU case, at low energy, in the quasi-harmonic limit, we find $\lambda_1(\varepsilon) \propto \varepsilon^2$. Whereas at high energy $\lambda_1(\varepsilon) \propto \varepsilon^{-1/6}$, here $\lambda_1(\varepsilon)$ is a decreasing function because at $\varepsilon \to \infty$ the systems is integrable. In an intermediate energy range our theoretical prediction underestimates the actual degree of chaoticity of the system. It is worth mentioning that this energy range coincides with a region of fully developed (strong) chaos detected in this model by a completely different approach in Ref. [31]. In this case – as already mentioned above – there was a-priori a reason to expect an inadequacy of the analytic prediction in some energy range. In fact, using Eisenhart metric, the explicit expression of the sectional curvature $K(v, \xi)$ – relative to the plane spanned by the velocity vector v and a generic vector $\xi \perp v$ (here we use ξ to denote the geodesic separation vector in order to avoid confusion with J which is the notation for the coupling constant) – is

$$K(v, \xi) = R_{0i0k} \frac{dq^0}{dt} \frac{\xi^i}{\|\xi\|} \frac{dq^0}{dt} \frac{\xi^k}{\|\xi\|} \equiv \frac{\partial^2 V}{\partial q^i \partial q^k} \frac{\xi^i \xi^k}{\|\xi\|^2} \ , \tag{98}$$

hence we get

$$K(v, \xi) = \frac{J}{\|\xi\|^2} \sum_{i=1}^{N} \cos(q_{i+1} - q_i) \left[\xi^{i+1} - \xi^i\right]^2 \tag{99}$$

for the coupled rotators model. We realize, by simple inspection of Eq. (99), that K can take negative values with non-vanishing probability regardless of the value of ε, whereas – as long as $\varepsilon < J$ – this possibility is lost in the replacement of K by Ricci curvature that we adopted in our theory. In fact, because of the constraint (88), at each point of the manifold it is

$$k_R(\varepsilon) \geq 2(J - \varepsilon) \tag{100}$$

thus our approximation fails in accounting for the presence of negative sectional curvatures at small values of ε. In Eq. (99) the cosines have different and variable weights, $[\xi^{i+1} - \xi^i]^2$, that in principle make possible to find somewhere along a geodesic $K < 0$ also with only one negative cosine. This is not the case of k_R where all the cosines have the same weight. Therefore the probability of finding $K < 0$ along a geodesic must be related to the probability of finding an angular difference greater than $\frac{\pi}{2}$ between two nearest-neighboring rotators. If the energy is sufficiently low this event will be very unlikely, but we can guess that it will become considerable where the theoretical prediction is not satisfactory, i.e. when chaos is strong. Notice that the frequent occurrence of $K < 0$ along a geodesic adds to parametric instability another instability mechanism that enforces chaos [Eq. (25)].

Our strategy is to modify the model for $K(s)$ in some *effective* way that takes into account the mentioned difficulty of $k_R(s)$ to adequately model $K(s)$. This will be achieved by suitably "renormalizing" Ω_0 or σ_Ω to obtain an *effective gaussian process* for the behavior of the sectional curvature.

From Eq. (99) we see that N directions of the vector ξ exist such that the sectional curvatures – relative to the N planes spanned by these vectors together with v – are just $\cos(q_{i+1} - q_i)$. Hence the probability $P(\varepsilon)$ of occurrence of a negative value of the cosine is used to estimate the probability of occurrence of negative sectional curvatures along the geodesics. This probability function has the following simple expression

$$P(\varepsilon) = \frac{\int_{-\pi}^{\pi} \Theta(-\cos x) e^{\beta J \cos x} dx}{\int_{-\pi}^{\pi} e^{\beta J \cos x} dx} = \frac{\int_{\frac{\pi}{2}}^{\frac{3\pi}{2}} e^{\beta J \cos x} dx}{2\pi I_0(\beta J)}, \tag{101}$$

where $\Theta(x)$ is the Heavyside unit step function.

The function $P(\varepsilon)$, reported in Fig. 7, begins to increase at $\varepsilon \simeq 0.2$, just where the analytic prediction in Fig. 6 begins to fail, and when it approaches its asymptotic value of $\frac{1}{2}$, around the end of the knee, a good agreement is again found between theory and numeric results. The simplest way to account for the existence of negative sectional curvatures is to

shift the peak of the distribution $\mathcal{P}(\delta K_R)$ toward the negative axis. This is achieved by the replacement

$$\langle k_R(\varepsilon) \rangle \rightarrow \frac{\langle k_R(\varepsilon) \rangle}{1 + \alpha P(\varepsilon)}. \tag{102}$$

This correction neither has influence when $P(\varepsilon) \simeq 0$ (below $\varepsilon \simeq 0.2$) nor when $P(\varepsilon) \simeq 1/2$ (because in this case $\langle k_R(\varepsilon) \rangle \rightarrow 0$). The value of the parameter α in (102) must be estimated *a posteriori* in order to obtain the best agreement between numerical and theoretical data over the whole range of energies. The result shown in Fig. 8 is obtained with $\alpha = 150$, anyhow no particularly fine tuning is necessary to obtain a very good agreement between theory and numerical experiment.

V. CONCLUDING REMARKS

The present paper contains a substantial progress along the research line initiated in Ref. [5] where it was proposed to tackle Hamiltonian chaos using the Riemannian geometrization of newtonian dynamics. This work renewed an old intuition that dates back to N. S. Krylov [11] and that spawned new ideas in abstract ergodic theory [12,16], whereas it did not give rise to any useful method to describe chaos in physical geodesic flows, despite of many attempts and with remarkable exceptions [13,14]. The obstacle was always the same: in analogy with Anosov flows, that live on hyperbolic manifolds, chaos has been invariably thought of as a consequence only of negative scalar curvature. So the first obvious check against any typical model that undergoes a stochastic transition – say the Hénon-Heiles model – gives a puzzling surprise: the scalar curvature of (M, g_J) is always positive [9] independently of the energy value, i.e. of regular or chaotic behavior of the dynamics.

The novelty of the approach started in Ref. [5] was to conjugate theoretical arguments with numerical experiments in order to shine some light on the following two points: *i)* does the geometry of the "mechanical" manifolds contain, though in some hidden way, the relevant information concerning stability and instability of their geodesics? and in the affirmative

31

case *ii)* how to quantify the strenght of chaos, how to characterize the weakly and strongly chaotic regimes?

Actually positive answers to these questions have been given in [5–10], where, among other things, it has been shown that if the geodesics feel a positive non-constant curvature of the underlying manifold then *parametric instability* can be activated. Though a rigorous proof is not yet at disposal, parametric instability appears as the source of chaos on manifolds of positive non-constant curvature.

By the way we can mention that also in the case of integrable systems, whose geodesics are therefore stable, the curvature of the underlying manifold can be wildly fluctuating along the geodesics but in this case the parametric instability mechanism is inactive, and it is found that these integrable geodesic flows have very special hidden symmetries, mathematically defined through Killing tensor fields [32], that make them peculiar.

For geodesic flows on constant negative curvature manifolds, the instability exponent is known [Eq. (25)], if the curvature is negative and non-constant then simple averaging algorithms can be devised, but what can we do with a positive and fluctuating curvature? The challenge was now to compute the average instability exponent for geodesic flows of physical relevance. This is a crucial test of effectiveness of the Riemannian theory of chaos with respect to the conventional explanation based on homoclinic intersections. Moreover, as no analytic method was available to compute Lyapunov exponents, it was worth making an effort in this direction.

Under reasonable hypotheses, that obviously restrict the domain of validity of the analytic formula (51) for λ_1, this paper provides the first analytic computations of the largest Lyapunov exponent in dynamical systems described by ordinary differential equations.

Though several points need a deeper understanding, we hope that our work convincingly shows that this geometric approach is effective and useful, thus deserving further improvements and developments.

APPENDIX A: SOLUTION OF THE STOCHASTIC OSCILLATOR EQUATION

In the following we will briefly describe how to cope with the stochastic oscillator problem which we encountered in Sec. III B. The discussion follows closely Van Kampen (Ref. [24]) where all the details can be found.

A stochastic differential equation can be put in the general form

$$F(x, \Omega) = 0, \tag{A1}$$

where F is an assigned function and the variable Ω is a random process, defined by a mean, a standard deviation and an autocorrelation function. A function $\xi(\Omega)$ is a solution of this equation if $\forall \Omega \; F(\xi(\Omega), \Omega) = 0$. If equation (A1) is linear of order n, it is written as

$$\dot{\mathbf{u}} = \mathbf{A}(t, \Omega)\mathbf{u} \tag{A2}$$

where $\mathbf{u} \in \mathbb{R}^n$ and $\mathbf{A}$ is a $n \times n$ matrix whose elements are randomly dependent on time.

For the purposes of our work we are interested in studying the evolution of the average carried over all the realizations of the process , $\langle \mathbf{u}(t) \rangle$. Let us consider the matrix $\mathbf{A}$ as the sum

$$\mathbf{A}(t, \Omega) = \mathbf{A}_0(t) + \alpha \mathbf{A}_1(t, \Omega) \tag{A3}$$

where the first term is Ω-independent and the second one is randomly fluctuating with zero mean. Let us also assume that $\mathbf{A}_0$ is time-independent. If the parameter α – that determines

the fluctuation amplitude – is small we can treat Eq. (A2) by means of a perturbation expansion. It is convenient to use the interaction picture, thus we put

$$\mathbf{u}(t) = \exp(\mathbf{A}_0 t)\mathbf{v}(t) \tag{A4}$$

$$\mathbf{A}_1(t) = \exp(\mathbf{A}_0 t)\mathbf{v}(t)\exp(-\mathbf{A}_0 t). \tag{A5}$$

Formally one is led to a Dyson expansion for the solution $\mathbf{v}(t)$. Then, going back to the previous variables and averaging, the second order approximation gives

$$\frac{d}{dt}\langle \mathbf{u}(t)\rangle = \{\mathbf{A}_0 + \alpha^2 \int_{-\infty}^{+\infty} \langle \mathbf{A}_1(t)\exp(\mathbf{A}_0\tau)\mathbf{A}_1(t-\tau)\rangle \exp(-\mathbf{A}_0\tau)d\tau\}\langle \mathbf{u}(t)\rangle \quad . \tag{A6}$$

Following the same procedure one can find also the evolution of the second moments (and by iterating also the evolution of higher moments). In fact, with the components of $\mathbf{u} \in \mathbb{R}^n$ we can make n^2 quantities $u_\nu u_\mu$ that obey the differential equation

$$\frac{d}{dt}(u_\nu u_\mu) = \sum_{k,\lambda} \tilde{A}_{\nu\mu,k\lambda}(t)(u_k u_\lambda), \tag{A7}$$

where

$$\tilde{A}_{\nu\mu,k\lambda} = A_{\nu k}\delta_{\mu\lambda} + \delta_{\nu k}A_{\mu\lambda} \quad . \tag{A8}$$

The above presented averaging method can be now applied to this new equation.

Now, if we consider a random harmonic oscillator, Eq. (A2) has the form

$$\frac{d}{dt}\begin{pmatrix} x \\ \dot{x} \end{pmatrix} = \begin{pmatrix} 0 & 1 \\ -\Omega & 0 \end{pmatrix}\begin{pmatrix} x \\ \dot{x} \end{pmatrix}, \tag{A9}$$

with the random squared frequency $\Omega = \Omega_0 + \sigma_\Omega \eta(t)$. In particular, we are interested in working out the second moments equation when the process $\eta(t)$ is gaussian and δ-correlated. Using Eq. (A8) one finds that

$$\frac{d}{dt}\begin{pmatrix} x^2 \\ \dot{x}^2 \\ x\dot{x} \end{pmatrix} = \begin{pmatrix} 0 & 0 & 2 \\ 0 & 0 & -2\Omega \\ -\Omega & 1 & 0 \end{pmatrix}\begin{pmatrix} x^2 \\ \dot{x}^2 \\ x\dot{x} \end{pmatrix} = \mathbf{A}\begin{pmatrix} x^2 \\ \dot{x}^2 \\ x\dot{x} \end{pmatrix} \quad . \tag{A10}$$

34

Because of our assumptions for this system, Eq. (A6) is more than a second order approximation, it is exact. In fact, the Dyson series can be written in compact form as

$$
\begin{pmatrix} \langle x^2(t) \rangle \\ \langle \dot{x}^2(t) \rangle \\ \langle x(t)\dot{x}(t) \rangle \end{pmatrix} = \lceil \langle \exp\left(\int_0^t \mathbf{A}(t')dt' \right) \rangle \rceil \begin{pmatrix} \langle x^2(0) \rangle \\ \langle \dot{x}^2(0) \rangle \\ \langle x(0)\dot{x}(0) \rangle \end{pmatrix}
\tag{A11}
$$

where the brackets $\lceil \ldots \rceil$ stand for a chronological product. According to Wick's procedure we can rewrite Eq. (A11) as a cumulant expansion, and when the cumulants of order higher than the second vanish (as is the case of interest to us) one can easily show that Eq. (A6) is exact.

Likewise in Eq. (A3), the matrix $\mathbf{A}$ splits as

$$
\mathbf{A}(t) = \mathbf{A}_0 + \sigma_\Omega \eta(t) \mathbf{A}_1 = \begin{pmatrix} 0 & 0 & 2 \\ 0 & 0 & -2\Omega_0 \\ -\Omega_0 & 1 & 0 \end{pmatrix} + \sigma_\Omega \eta(t) \begin{pmatrix} 0 & 0 & 0 \\ 0 & 0 & -2 \\ -1 & 0 & 0 \end{pmatrix}
\tag{A12}
$$

therefore the equation for the averages becomes

$$
\frac{d}{dt} \begin{pmatrix} \langle x^2 \rangle \\ \langle \dot{x}^2 \rangle \\ \langle x\dot{x} \rangle \end{pmatrix} = \{ \mathbf{A}_0 + \sigma_\Omega^2 \int_{-\infty}^{+\infty} \langle \eta(t)\eta(t-\tau) \rangle \mathbf{B}(\tau)d\tau \} \begin{pmatrix} \langle x^2 \rangle \\ \langle \dot{x}^2 \rangle \\ \langle x\dot{x} \rangle \end{pmatrix},
\tag{A13}
$$

where $\mathbf{B}(\tau) = \mathbf{A}_1 \exp(\mathbf{A}_0 \tau) \mathbf{A}_1 \exp(-\mathbf{A}_0 \tau)$. As $\langle \eta(t)\eta(t-\tau) \rangle = \tau\delta(\tau)$, with τ a characteristic time scale of the process, we obtain

$$
\frac{d}{dt} \begin{pmatrix} \langle x^2 \rangle \\ \langle \dot{x}^2 \rangle \\ \langle x\dot{x} \rangle \end{pmatrix} = \{ \mathbf{A}_0 + \sigma_\Omega^2 \tau \mathbf{B}(0) \} \begin{pmatrix} \langle x^2 \rangle \\ \langle \dot{x}^2 \rangle \\ \langle x\dot{x} \rangle \end{pmatrix} .
\tag{A14}
$$

From the definition of $\mathbf{B}(\tau)$ it follows that $\mathbf{B}(0) = \mathbf{A}_1^2$, then by easy calculations we find

$$
\mathbf{A}_0 + \sigma_\Omega^2 \tau \mathbf{A}_1^2 = \begin{pmatrix} 0 & 0 & 2 \\ 2\sigma_\Omega^2 \tau & 0 & -2\Omega_0 \\ -\Omega_0 & 1 & 0 \end{pmatrix}
\tag{A15}
$$

which is the result used in Sec. III B.

REFERENCES

*   Also at INFN, sezione di Firenze, Italy. E-mail: casetti@sns.it

†   Also at INFM, unità di Trieste, and INFN, sezione di Trieste, Italy. E-mail: clementi@sissa.it

‡   Also at INFM, unità di Firenze, and INFN, sezione di Firenze, Italy. E-mail: pettini@arcetri.astro.it

[1] This definition can be extended also to quantum systems, see G. Iacomelli and M. Pettini, Phys. Lett. A **212**, 29 (1996).

[2] In the paper: E.Gozzi and M. Reuter, Chaos, Solitons & Fractals **4**, 1117 (1994), the authors show the connection between Lyapunov exponents and supersymmetry through a path-integral formulation of both stochastic and deterministic dynamics. This is a very interesting approach because Lyapunov exponents are represented as expectation values of some observables, thus in principle they can be computed by means of standard field-theoretic methods. However – at present – there are no examples of how the method might work in practice.

[3] M. Pettini and M. Landolfi, Phys. Rev. A **41**, 768 (1990).

[4] M. Pettini and M. Cerruti-Sola, Phys. Rev. A **44**, 975 (1991).

[5] M. Pettini, Phys. Rev. E **47**, 828 (1993).

[6] L. Casetti and M. Pettini, Phys. Rev. E **48**, 4320 (1993).

[7] L. Casetti, R. Livi, and M. Pettini, Phys. Rev. Lett. **74**, 375 (1995).

[8] M. Cerruti-Sola and M. Pettini, Phys. Rev. E **51**, 53 (1995).

[9] M. Cerruti-Sola and M. Pettini, Phys. Rev. E **53**, 179 (1996).

[10] M. Pettini and R. Valdettaro, Chaos **5**, 646 (1995).

[11] N. S. Krylov, *Works on the Foundations of Statistical Physics*, (Princeton University Press, Princeton, 1979), here a reprint of his doctoral thesis of 1942 can be found.

[12] *ibidem*, Ya. G. Sinai, *Development of Krylov's ideas*.

[13] A. Knauf, Comm. Math. Phys. **110**, 89 (1987).

[14] M. C. Gutzwiller, J. Math. Phys. **18**, 806 (1977), and earlier works by the same author quoted therein.

[15] L. P. Eisenhart, Ann. Math. **30**, 591 (1929).

[16] D. V. Anosov, Proc. Steklov Math. Inst. **90**, 1 (1967). See for a review Ya. G. Sinai, *Dynamical Systems II*, Encyclopædia of Mathematical Sciences Vol. 2 (Springer-Verlag, Berlin, 1989).

[17] A. H. Nayfeh and D. T. Mook, *Nonlinear Oscillations* (Wiley, New York, 1979).

[18] S. I. Goldberg, *Curvature and Homology* (Dover, New York, 1965).

[19] M. P. Do Carmo, *Riemannian Geometry* (Birkhäuser, Boston, 1992).

[20] At $N \geq 3$, after the Poincaré-Fermi theorem, generic nonintegrable systems have no smooth invariant besides energy, thus the whole constant energy surface is topologically accessible. One might think that troubles with ergodicity could be raised by the KAM theorem, but at large N this is not possible because a positive measure of tori survives a perturbation of amplitude smaller than some threshold value, and the threshold typically drops to zero as $\exp(-cN \ln N)$, c is a constant.

[21] The conjugate points are defined by the vanishing of Jacobi field of geodesic separation.

[22] A subset $\mathcal{M}$ of a Riemannian manifold is said to be strongly convex if every minimal geodesic joining two of its points always lies in $\mathcal{M}$. The lowering of the bound follows from a theorem due to Whitehead, see: J. Cheeger, D. G. Ebin, *Comparison theorems in Riemannian geometry* (North Holland, Amsterdam, 1975).

[23] This is a consequence of the possibility of approximating locally the metric of a manifold by $g_{ik} \simeq \delta_{ik} - \frac{1}{6} R_{ikjl} u^i u^k$ obtained by using normal coordinates and displacements u^i (see e.g. Do Carmo, Ref. [19]).

[24] N. G. Van Kampen, Phys. Rep. **24**, 71 (1976).

[25] E. Fermi, J. Pasta, and S. Ulam, Los Alamos Report LA-1940 (1955), in E. Segré (ed.), *Collected Papers of Enrico Fermi*, (University of Chicago, Chicago, 1965), Vol. 2, p. 978.

[26] J. Ford, Phys. Rep. **213**, 271 (1992).

[27] J. L. Lebowitz, J. K. Percus, and L. Verlet, Phys. Rev. **153**, 250 (1967).

[28] R. Livi, M. Pettini, S. Ruffo, and A. Vulpiani, J. Stat. Phys. **48**, 539 (1987).

[29] L. Casetti, Physica Scripta **51**, 29 (1995).

[30] G. Benettin, L. Galgani, and J.-M. Strelcyn, Phys. Rev. A **14**, 2338 (1976); G. Benettin, L. Galgani, A. Giorgilli, and J.-M. Strelcyn, Meccanica **15**, 9 and 21 (1980). See also A. J. Lichtenberg and M. A. Lieberman, *Regular and Chaotic Dynamics*, 2nd edition (Springer-Verlag, Berlin, 1992).

[31] D. Escande, H. Kantz, R. Livi, and S. Ruffo, J. Stat. Phys. **76**, 605 (1994).

[32] C. Clementi, Laurea Thesis in Physics, Università di Firenze, Italy (1995).

FIGURES

FIG. 1. Average Ricci curvature $\langle k_R \rangle$ vs. energy density ε for the FPU model: comparison between analytic computation with Eq. (74) (solid line) and the outcome of numerical simulations (time averages) with $N = 128$ (solid circles) and $N = 512$ (solid triangles); $\mu = 0.1$.

FIG. 2. Fluctuation of Ricci curvature $\langle \delta^2 K_R \rangle / N$ vs. energy density ε for the FPU model: comparison between analytic computation with Eq. (82) (solid line) and numerical results. Symbols and parameters as in Fig. 1.

FIG. 3. Lyapunov exponent λ_1 vs. energy density ε for the FPU model: comparison between theoretical prediction of Eq. (51) (solid line) and numerical estimates at $N = 256$ (solid circles) and $N = 2000$ (solid squares); $\mu = 0.1$.

FIG. 4. Average Ricci curvature $\langle k_R \rangle$ vs. energy density ε for the coupled rotators model: comparison between analytic computation with Eq. (92) (solid line) and the outcome of numerical simulations (time averages) with $N = 150$ (solid circles); $J = 1$.

FIG. 5. Fluctuation of Ricci curvature $\langle \delta^2 K_R \rangle / N$ vs. energy density ε for the FPU model: comparison between analytic computation with Eq. (97) (solid line) and numerical results. Symbols and parameters as in Fig. 4.

FIG. 6. Lyapunov exponent λ_1 vs. energy density ε for the coupled rotators model: comparison between theoretical prediction of Eq. (51) (solid line) and numerical estimates at $N = 150$ (solid circles), $N = 1000$ (solid rhombs) and $N = 1500$ (solid square); $J = 1$.

FIG. 7. Estimate of the probability $P(\varepsilon)$ of occurrence of negative sectional curvatures in the coupled rotators model according to Eq. (101); $J = 1$.

FIG. 8. Lyapunov exponent λ_1 vs. energy density ε for the coupled rotators model: comparison between theoretical prediction and numerical estimates as in Fig. 6, but here the average curvature $\langle k_R \rangle$ which enters Eq. (51) is corrected according to Eq. (102) with $\alpha = 150$. Numerical values of λ_1 are obtained at $N = 150$ (solid circles), at $N = 1000$ (solid rhombs) and at $N = 1500$ (solid square).

FIG.1 Casetti et al.
''Riemannian theory of Hamiltonian chaos...''
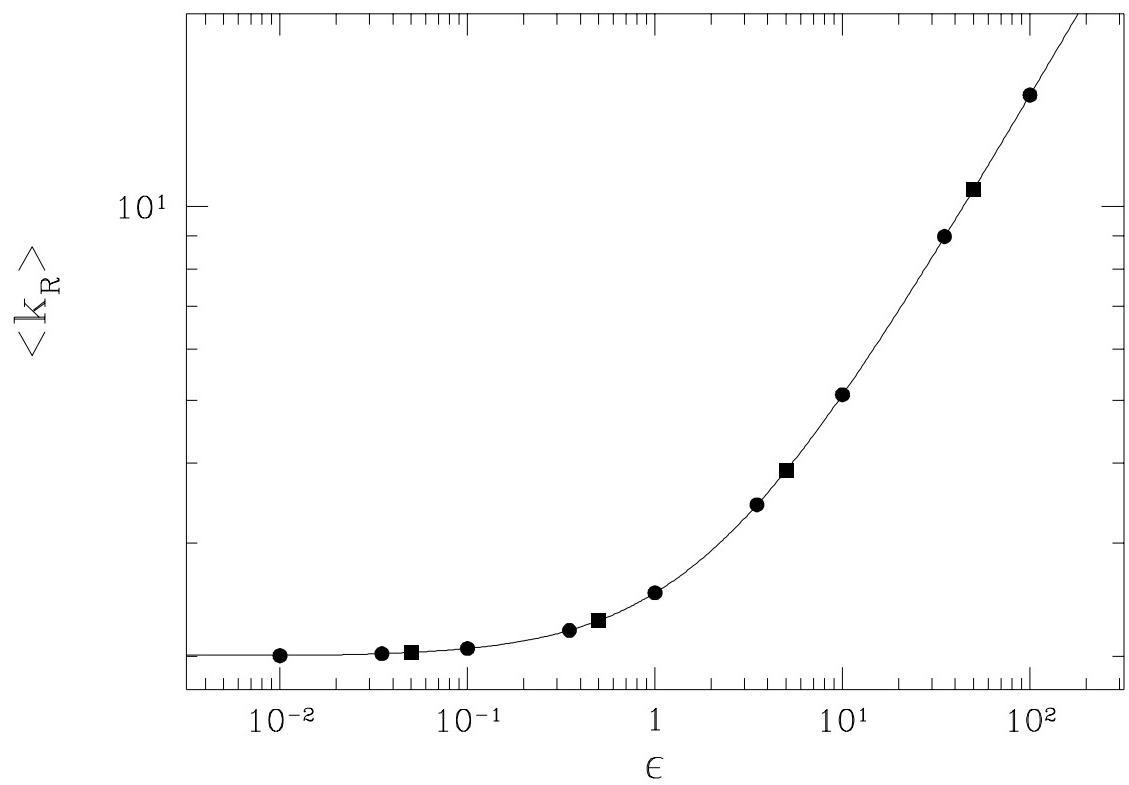
FIG.2 Casetti et al.
"Riemannian theory of Hamiltonian chaos..."
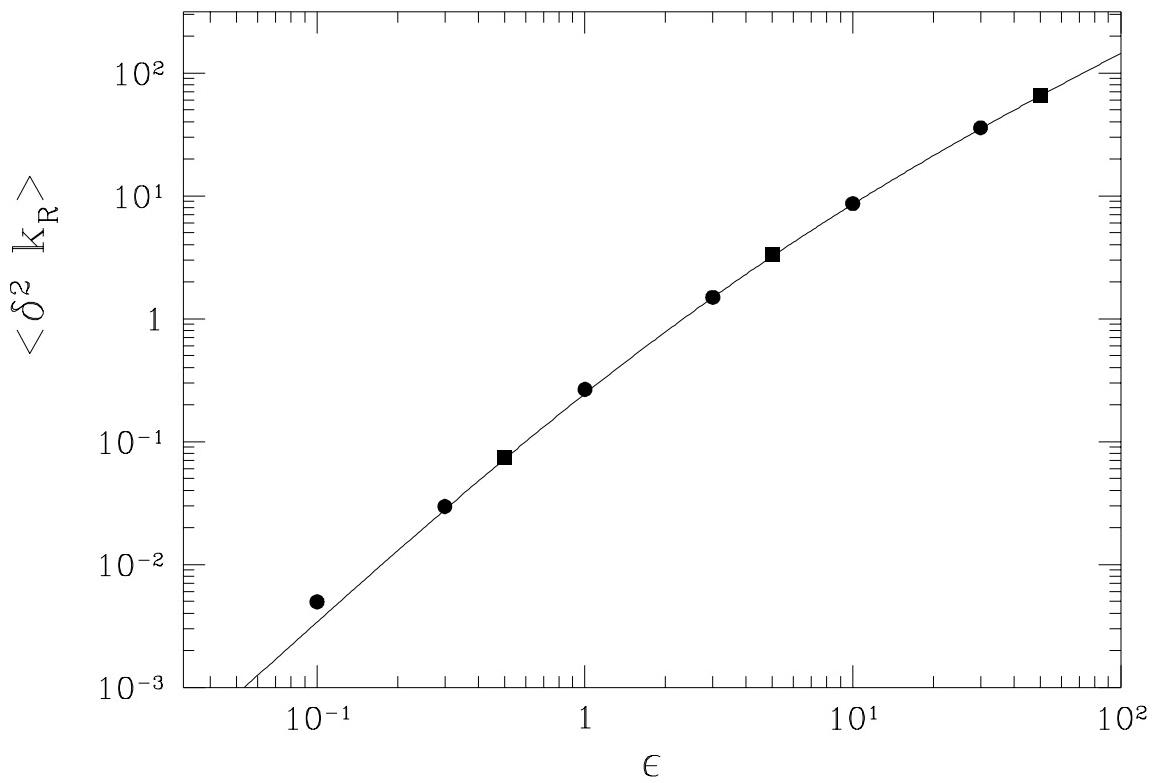
FIG.3 Casetti et al.
"Riemannian theory of Hamiltonian chaos..."
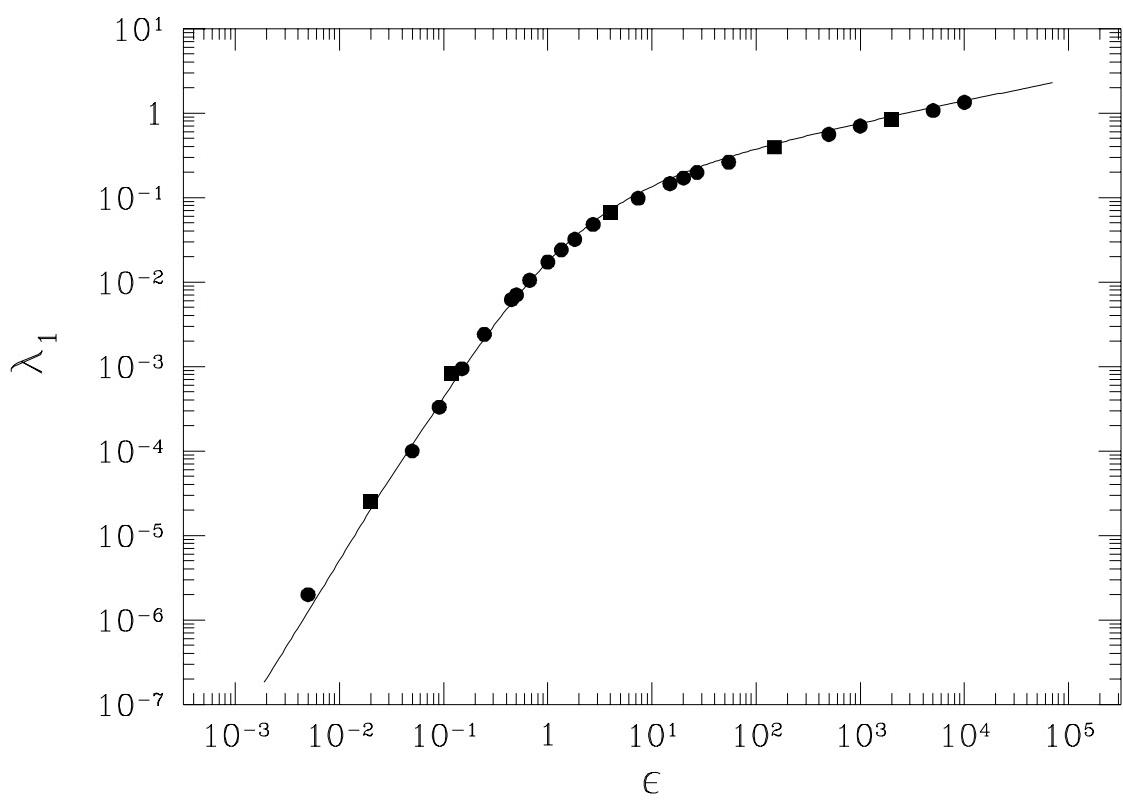
FIG.4 Casetti et al.
''Riemannian theory of Hamiltonian chaos...''
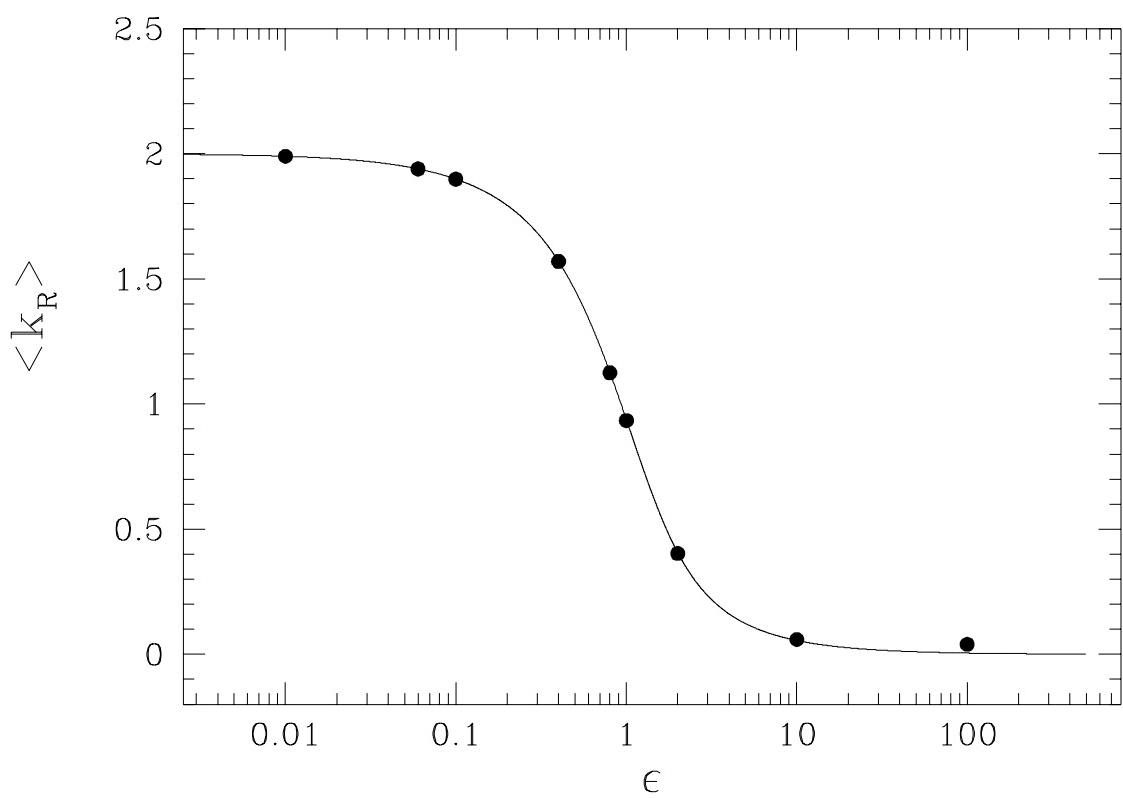
FIG.5 Casetti et al.
''Riemannian theory of Hamiltonian chaos...''
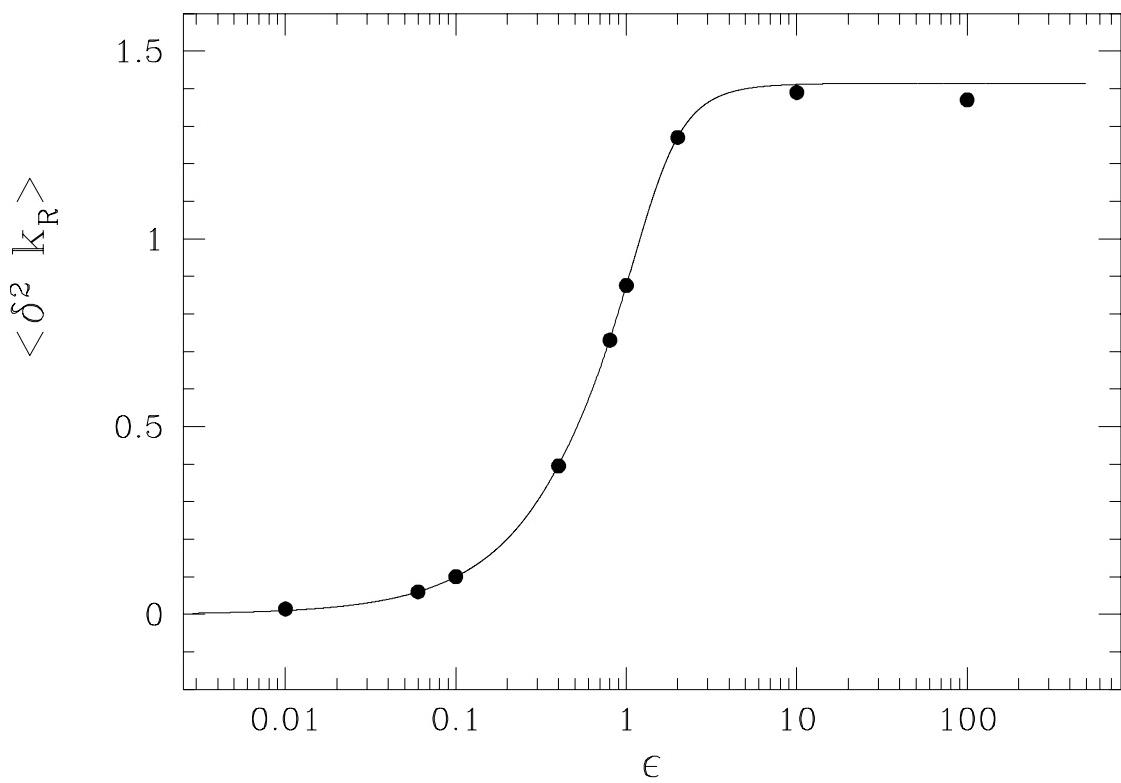
FIG 6 Casetti et al.
"Riemannian theory of Hamiltonian chaos..."
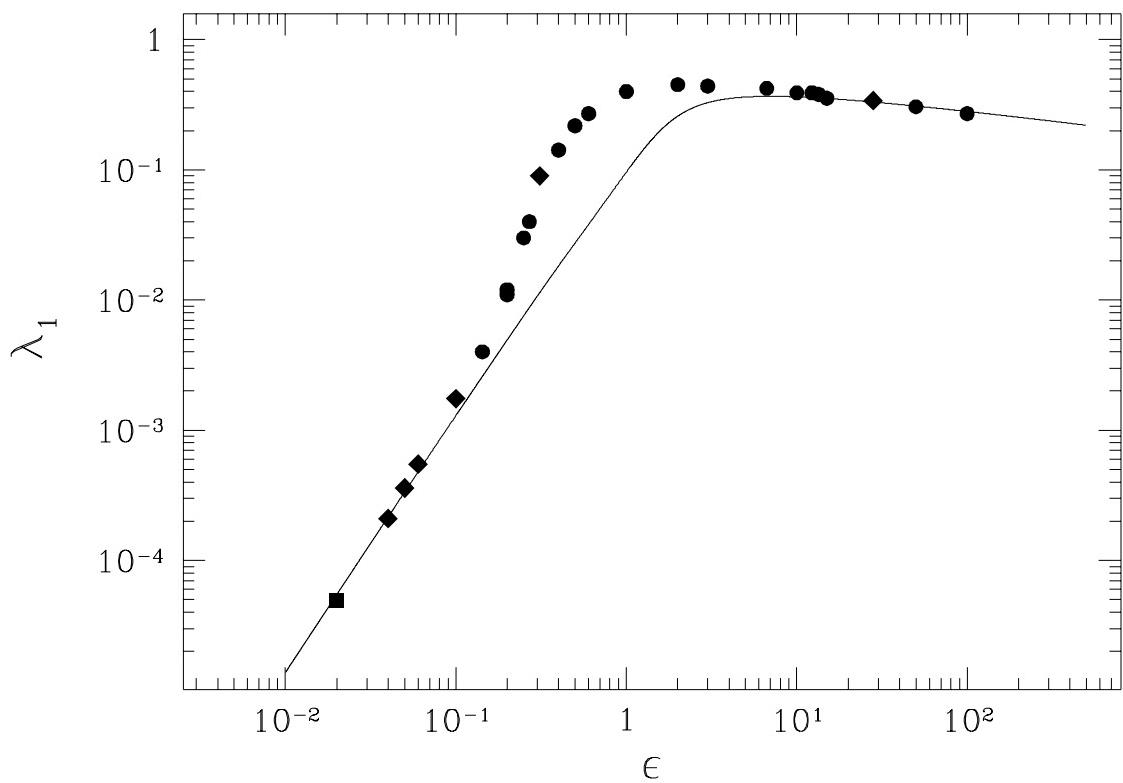
FIG.7 Casetti et al.
''Riemannian theory of Hamiltonian chaos...''

FIG.8 Casetti et al.
''Riemannian theory of Hamiltonian chaos...''